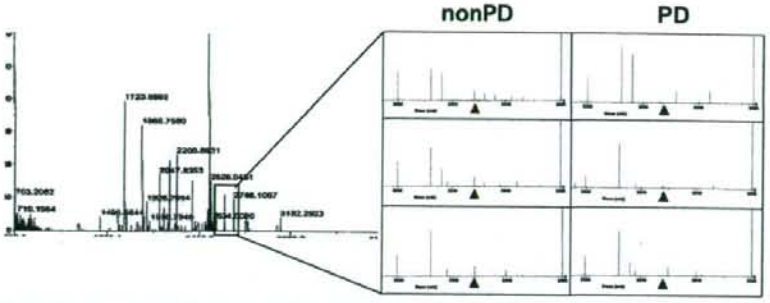

Figure 3. Representative data of plasma N-glycan profile measured using MALDI-TOF-MS (left panel). Twenty-seven microliters of plasma sample was used for the analysis. The mixture was trypsinized and reacted using *N*-glycosidase F. Internal N-glycan standard was added, and the mixture was purified using glycoblotting-based glycan enrichment. The purified samples were measured using MALDI-TOF-MS in reflector, positive ion mode. The number of laser shots was 300 × 2 shots, and the mass range acquired was 700–5000 Da. The N-glycan structure was determined using the GlycoSuite online database, proteome System. All the plasma N-glycans peaks obtained from MALDI-TOF-MS were normalized using the internal standard. The identified 2534 *m/z* N-glycan peaks are shown in six plasma samples (right panel). ▲, 2534 *m/z*; PD, progressive disease.

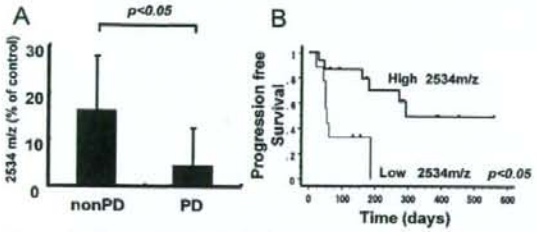

Figure 4. Plasma 2534 *m/z* N-glycan and clinical outcome. (A) Expression of plasma 2534 *m/z* N-glycan and clinical response. The expression of plasma 2534 *m/z* N-glycan was significantly lower ($p < 0.05$) in patients with progressive disease (PD). (B) Kaplan–Meier curve of high (detectable) or low (not detectable) plasma 2534 *m/z* N-glycan groups for progression-free survival (PFS) after trastuzumab treatment. The patients with a low expression of plasma 2534 *m/z* N-glycan exhibited a significantly shorter PFS ($p < 0.05$).

using a serum samples, and cancer biopsy specimens are not needed. In the present study, when the plasma N-glycan profiles of breast cancer patients were examined using MALDI-TOF-MS, 2534 *m/z* N-glycan was found to be correlated with clinical response and PFS. The estimated structure of the identified 2534 *m/z* N-glycan is (Hex)5(HexNAc)2(Deoxyhexose)1 + (Man)3(GlcNAc)2 according to a database (http://au.expasy.org/tools/glycomod/). The experimental confirmation of the predicted structure of 2534 *m/z* is very important. Although we no longer have enough plasma samples to determine the experimental confirmation of structure, we plan to examine 2534 N-glycan in clinical samples to give the experimental confirmation in the future prospective study. This N-glycan has also been found in plasma samples from patients with pancreas cancer, pancreatitis and obstructive bile duct disease (data not shown). We are now investigating the biological mechanism of this N-glycan modification.

In conclusion, we demonstrated that plasma FUCA activity and plasma N-glycan are correlated with the clinical outcome of breast cancer patients treated with trastuzumab. N-Glycan profiles raise the possibility of identifying novel predictive biomarkers for antibody therapy, although a validation study with a larger sample size is needed. Our results show the utility of glycosylation analysis for clinical cancer therapy and provide a novel insight into biomarker studies using glycobiological tools in the field of breast cancer.

Acknowledgment. The following people have played very important roles in the outcome of this project: Hisao Fukumoto, Tatsu Shimoyama, Naoki Hayama, Hideharu Kimura, Masayuki Takeda, Junya Fukai, Kazuko Sakai and Terufumi Kato. We also thank Dr. Richard Simon and Dr. Amy Peng for providing the BRB ArrayTools software. We thank Mr. Hideyuki Shimaoka and Mr. Kazuhiko Fujiwara (Sumitomo Bakelite Co., Ltd.) for their technical support and useful advice. We also thank Mrs. Eiko Honda (Life Science Research Institute, Kinki University) for assistance with the experiments. This work was supported by funds for Health and Labor Scientific Research Grants, Research on Advanced Medical Technology H17-Pharmaco-006 and for the Third-Term Comprehensive 10-Year Strategy for Cancer Control. K.M. is the recipient of a Research Resident Fellowship from the Foundation of Promotion of Cancer Research in Japan.

References

(1) Hakomori, S. Glycosylation defining cancer malignancy: new wine in an old bottle. *Proc. Natl. Acad. Sci. U.S.A.* **2002**, *99* (16), 10231–3.

(2) Ono, M.; Hakomori, S. Glycosylation defining cancer cell motility and invasiveness. *Glycoconjugate J.* **2004**, *20* (1), 71–8.

(3) Zhao, Y. Y.; Takahashi, M.; Gu, J. G.; Miyoshi, E.; Matsumoto, A.; Kitazume, S.; Taniguchi, N. Functional roles of N-glycans in cell signaling and cell adhesion in cancer. *Cancer Sci.* **2008**, *99* (7), 1304–10.

(4) Hakomori, S. Tumor malignancy defined by aberrant glycosylation and sphingo(glyco)lipid metabolism. *Cancer Res.* **1996**, *56* (23), 5309–18.

(5) Contessa, J. N.; Bhojani, M. S.; Freeze, H. H.; Rehemtulla, A.; Lawrence, T. S. Inhibition of N-linked glycosylation disrupts receptor tyrosine kinase signaling in tumor cells. *Cancer Res.* **2008**, *68* (10), 3803–9.

(6) Guo, H. B.; Randolph, M.; Pierce, M. Inhibition of a specific N-glycosylation activity results in attenuation of breast carcinoma cell invasiveness-related phenotypes: inhibition of epidermal growth factor-induced dephosphorylation of focal adhesion kinase. *J. Biol. Chem.* **2007**, *282* (30), 22150–62.

(7) Qiu, Y.; Patwa, T. H.; Xu, L.; Shedden, K.; Misek, D. E.; Tuck, M.; Jin, G.; Ruffin, M. T.; Turgeon, D. K.; Synal, S.; Bresalier, R.; Marcon, N.; Brenner, D. E.; Lubman, D. M. Plasma glycoprotein profiling for colorectal cancer biomarker identification by lectin glycoarray and lectin blot. *J. Proteome Res.* **2008**, *7* (4), 1693–703.

(8) Abbott, K. L.; Aoki, K.; Lim, J. M.; Porterfield, M.; Johnson, R.; O'Regan, R. M.; Wells, L.; Tiemeyer, M.; Pierce, M. Targeted glycoproteomic identification of biomarkers for human breast carcinoma. *J. Proteome Res.* **2008**, *7* (4), 1470–80.
(9) Heo, S. H.; Lee, S. J.; Ryoo, H. M.; Park, J. Y.; Cho, J. Y. Identification of putative serum glycoprotein biomarkers for human lung adenocarcinoma by multilectin affinity chromatography and LC-MS/MS. *Proteomics* **2007**, *7* (23), 4292–302.
(10) Nakagawa, T.; Uozumi, N.; Nakano, M.; Mizuno-Horikawa, Y.; Okuyama, N.; Taguchi, T.; Gu, J.; Kondo, A.; Taniguchi, N.; Miyoshi, E. Fucosylation of N-glycans regulates the secretion of hepatic glycoproteins into bile ducts. *J. Biol. Chem.* **2006**, *281* (40), 29797–806.
(11) Ueda, K.; Katagiri, T.; Shimada, T.; Irie, S.; Sato, T. A.; Nakamura, Y.; Daigo, Y. Comparative profiling of serum glycoproteome by sequential purification of glycoproteins and 2-nitrobenzensulfenyl (NBS) stable isotope labeling: a new approach for the novel biomarker discovery for cancer. *J. Proteome Res.* **2007**, *6* (9), 3475–83.
(12) Li, D.; Mallory, T.; Satomura, S. AFP-L3: a new generation of tumor marker for hepatocellular carcinoma. *Clin. Chim. Acta* **2001**, *313* (1–2), 15–9.
(13) Yamaguchi, Y.; Fujii, J.; Inoue, S.; Uozumi, N.; Yanagidani, S.; Ikeda, Y.; Egashira, M.; Miyoshi, O.; Niikawa, N.; Taniguchi, N. Mapping of the alpha-1,6-fucosyltransferase gene, FUT8, to human chromosome 14q24.3. *Cytogenet. Cell Genet.* **1999**, *84* (1–2), 58–60.
(14) Yamane-Ohnuki, N.; Kinoshita, S.; Inoue-Urakubo, M.; Kusunoki, M.; Iida, S.; Nakano, R.; Wakitani, M.; Niwa, R.; Sakurada, M.; Uchida, K.; Shitara, K.; Satoh, M. Establishment of FUT8 knockout Chinese hamster ovary cells: an ideal host cell line for producing completely defucosylated antibodies with enhanced antibody-dependent cellular cytotoxicity. *Biotechnol. Bioeng.* **2004**, *87* (5), 614–22.
(15) Niwa, R.; Hatanaka, S.; Shoji-Hosaka, E.; Sakurada, M.; Kobayashi, Y.; Uehara, A.; Yokoi, H.; Nakamura, K.; Shitara, K. Enhancement of the antibody-dependent cellular cytotoxicity of low-fucose IgG1 is independent of FcgammaRIIIa functional polymorphism. *Clin. Cancer Res.* **2004**, *10* (18 Pt 1), 6248–55.
(16) Suzuki, E.; Niwa, R.; Saji, S.; Muta, M.; Hirose, M.; Iida, S.; Shiotsu, Y.; Satoh, M.; Shitara, K.; Kondo, M.; Toi, M. A nonfucosylated anti-HER2 antibody augments antibody-dependent cellular cytotoxicity in breast cancer patients. *Clin. Cancer Res.* **2007**, *13* (6), 1875–82.
(17) Giardina, M. G.; Matarazzo, M.; Morante, R.; Lucariello, A.; Varriale, A.; Guardasole, V.; De Marco, G. Serum alpha-L-fucosidase activity and early detection of hepatocellular carcinoma: a prospective study of patients with cirrhosis. *Cancer.* **1998**, *83* (12), 2468–74.
(18) Ayude, D.; Paez De La Cadena, M.; Martinez-Zorzano, V. S.; Fernandez-Briera, A.; Rodriguez-Berrocal, F. J. Preoperative serum alpha-L-fucosidase activity as a prognostic marker in colorectal cancer. *Oncology* **2003**, *64* (1), 36–45.
(19) Ayude, D.; Fernandez-Rodriguez, J.; Rodriguez-Berrocal, F. J.; Martinez-Zorzano, V. S.; de Carlos, A.; Gil, E.; Paez de La Cadena, M. Value of the serum alpha-L-fucosidase activity in the diagnosis of colorectal cancer. *Oncology* **2000**, *59* (4), 310–6.
(20) Slamon, D. J.; Clark, G. M.; Wong, S. G.; Levin, W. J.; Ullrich, A.; McGuire, W. L. Human breast cancer: correlation of relapse and survival with amplification of the HER-2/neu oncogene. *Science* **1987**, *235* (4785), 177–82.
(21) Seshadri, R.; Firgaira, F. A.; Horsfall, D. J.; McCaul, K.; Setlur, V.; Kitchen, P. Clinical significance of HER-2/neu oncogene amplification in primary breast cancer. The South Australian Breast Cancer Study Group. *J Clin Oncol.* **1993**, *11* (10), 1936–42.
(22) Menard, S.; Pupa, S. M.; Campiglio, M.; Tagliabue, E. Biologic and therapeutic role of HER2 in cancer. *Oncogene* **2003**, *22* (42), 6570–8.
(23) Vogel, C. L.; Cobleigh, M. A.; Tripathy, D.; Gutheil, J. C.; Harris, L. N.; Fehrenbacher, L.; Slamon, D. J.; Murphy, M.; Novotny, W. F.; Burchmore, M.; Shak, S.; Stewart, S. J.; Press, M. Efficacy and safety of trastuzumab as a single agent in first-line treatment of HER2-overexpressing metastatic breast cancer. *J. Clin. Oncol.* **2002**, *20* (3), 719–26.
(24) Hurley, J.; Doliny, P.; Reis, I.; Silva, O.; Gomez-Fernandez, C.; Velez, P.; Pauletti, G.; Powell, J. E.; Pegram, M. D.; Slamon, D. J. Docetaxel, cisplatin, and trastuzumab as primary systemic therapy for human epidermal growth factor receptor 2-positive locally advanced breast cancer. *J. Clin. Oncol.* **2006**, *24* (12), 1831–8.
(25) Naruse, I.; Fukumoto, H.; Saijo, N.; Nishio, K. Enhanced anti-tumor effect of trastuzumab in combination with cisplatin. *Jpn. J. Cancer Res.* **2002**, *93* (5), 574–81.
(26) Kimura, H.; Sakai, K.; Arao, T.; Shimoyama, T.; Tamura, T.; Nishio, K. Antibody-dependent cellular cytotoxicity of cetuximab against tumor cells with wild-type or mutant epidermal growth factor receptor. *Cancer Sci.* **2007**, *98* (8), 1275–80.
(27) Kimura, H.; Kasahara, K.; Kawaishi, M.; Kunitoh, H.; Tamura, T.; Holloway, B.; Nishio, K. Detection of epidermal growth factor receptor mutations in serum as a predictor of the response to gefitinib in patients with non-small-cell lung cancer. *Clin. Cancer Res.* **2006**, *12* (13), 3915–21.
(28) Arao, T.; Fukumoto, H.; Takeda, M.; Tamura, T.; Saijo, N.; Nishio, K. Small in-frame deletion in the epidermal growth factor receptor as a target for ZD6474. *Cancer Res.* **2004**, *64* (24), 9101–4.
(29) Matsumoto, K.; Yokote, H.; Arao, T.; Maegawa, M.; Tanaka, K.; Fujita, Y.; Shimizu, C.; Hanafusa, T.; Fujiwara, Y.; Nishio, K. N-Glycan fucosylation of epidermal growth factor receptor modulates receptor activity and sensitivity to epidermal growth factor receptor tyrosine kinase inhibitor. *Cancer Sci.* **2008**, *99* (8), 1611–17.
(30) Uozumi, N.; Teshima, T.; Yamamoto, T.; Nishikawa, A.; Gao, Y. E.; Miyoshi, E.; Gao, C. X.; Noda, K.; Islam, K. N.; Ihara, Y.; Fujii, S.; Shiba, T.; Taniguchi, N. A fluorescent assay method for GDP-L-Fuc:N-acetyl-beta-D-glucosaminide alpha 1–6fucosyltransferase activity, involving high performance liquid chromatography. *J. Biochem.* **1996**, *120* (2), 385–92.
(31) Miura, Y.; Hato, M.; Shinohara, Y.; Kuramoto, H.; Furukawa, J.; Kurogochi, M.; Shimaoka, H.; Tada, M.; Nakanishi, K.; Ozaki, M.; Todo, S.; Nishimura, S. BlotGlycoABCTM, an integrated glycoblotting technique for rapid and large scale clinical glycomics. *Mol. Cell. Proteomics* **2008**, *7* (2), 370–7.
(32) Shah, M.; Telang, S.; Raval, G.; Shah, P.; Patel, P. S. Serum fucosylation changes in oral cancer and oral precancerous conditions: alpha-L-fucosidase as a marker. *Cancer* **2008**, *113* (2), 336–46.
(33) Ng, W. G.; Donnell, G. N.; Koch, R.; Bergren, W. R. Biochemical and genetic studies of plasma and leukocyte alpha-L-fucosidase. *Am. J. Hum. Genet.* **1976**, *28* (01), 42–50.
(34) Zhao, J.; Qiu, W.; Simeone, D. M.; Lubman, D. M. N-linked glycosylation profiling of pancreatic cancer serum using capillary liquid phase separation coupled with mass spectrometric analysis. *J. Proteome Res.* **2007**, *6* (3), 1126–38.
(35) Zhao, J.; Simeone, D. M.; Heidt, D.; Anderson, M. A.; Lubman, D. M. Comparative serum glycoproteomics using lectin selected sialic acid glycoproteins with mass spectrometric analysis: application to pancreatic cancer serum. *J. Proteome Res.* **2006**, *5* (7), 1792–802.
(36) Isailovic, D.; Kurulugama, R. T.; Plasencia, M. D.; Stokes, S. T.; Kyselova, Z.; Goldman, R.; Mechref, Y.; Novotny, M. V.; Clemmer, D. E. Profiling of human serum glycans associated with liver cancer and cirrhosis by IMS-MS. *J. Proteome Res.* **2008**, *7* (3), 1109–17.
(37) Kyselova, Z.; Mechref, Y.; Kang, P.; Goetz, J. A.; Dobrolecki, L. E.; Sledge, G. W.; Schnaper, L.; Hickey, R. J.; Malkas, L. H.; Novotny, M. V. Breast cancer diagnosis and prognosis through quantitative measurements of serum glycan profiles. *Clin Chem.* **2008**, *54* (7), 1166–75.
(38) An, H. J.; Miyamoto, S.; Lancaster, K. S.; Kirmiz, C.; Li, B.; Lam, K. S.; Leiserowitz, G. S.; Lebrilla, C. B. Profiling of glycans in serum for the discovery of potential biomarkers for ovarian cancer. *J. Proteome Res.* **2006**, *5* (7), 1626–35.

PR800655P

Available online at www.sciencedirect.com
ScienceDirect
Cancer Letters 270 (2008) 260–268
CANCER Letters
www.elsevier.com/locate/canlet

Antiangiogenic cancer therapy using tumor vasculature-targeted liposomes encapsulating 3-(3,5-dimethyl-1H-pyrrol-2-ylmethylene)-1,3-dihydro-indol-2-one, SU5416

Yasufumi Katanasaka [a,b], Tomoko Ida [a], Tomohiro Asai [a], Kosuke Shimizu [a], Fumiaki Koizumi [b], Noriyuki Maeda [c], Kazuhiko Baba [d], Naoto Oku [a,*]

[a] *Department of Medical Biochemistry, School of Pharmaceutical Sciences and Global COE, University of Shizuoka, 52-1 Yada, Suruga-ku, Shizuoka 422-8526, Japan*
[b] *Shien-Lab Medical Oncology Department, National Cancer Center Hospital, 5-1-1 Tsukiji, Chuo-ku, Tokyo 104-0045, Japan*
[c] *Nippon Fine Chemical Co., Ltd., Takasago, Hyogo 676-0074, Japan*
[d] *Taiho Pharmaceutical Co., Ltd., Kawauchi-cho, Tokushima 771-0194, Japan*

Received 21 February 2008; received in revised form 21 February 2008; accepted 8 May 2008

Abstract

Previously, we identified angiogenic vessel-homing peptide Ala-Pro-Arg-Pro-Gly (APRPG), and showed that APRPG-modified liposomes could selectively target to tumor neovasculature. Here, we designed an APRPG-modified liposome encapsulating SU5416, an angiogenesis inhibitor, to overcome the solubility problem, and to enhance the antiangiogenic activity of SU5416. Liposomal SU5416 appeared to have the appropriate characteristics, such as particle size and stability in serum. It showed a significantly lower hemoglobin release than SU5416 dissolved in a Cremophor EL-containing solvent. Compared with peptide-unmodified liposomal SU5416, the APRPG-modified liposomal SU5416 significantly suppressed tumor growth and with no remarkable side effects. Thus, targeted delivery of antiangiogenic drugs with tumor vasculature-targeted liposomes may be useful for antiangiogenic cancer therapy.

Keywords: Angiogenesis; Drug delivery systems; SU5416; Antiangiogenic therapy; APRPG-modified liposomes

1. Introduction

Angiogenesis is the development of new blood vessels from pre-existing vessels, and is an attractive target for cancer therapy because it is essential for tumor growth and hematogenous metastasis [1]. Vascular targeting therapy is divided into two main types: (i) antiangiogenic approach, which prevents the processes of angiogenesis in tumors, through inhibitors of angiogenic signaling; and (ii) antivascular approach, which impairs the established neovasculature using a vascular disrupt agent [2].

Vascular endothelial growth factor (VEGF) and its receptors are the best-characterized signal pathway in angiogenesis and are regarded as a target molecule for the antiangiogenic approach [3]. In

* Corresponding author. Tel.: +81 54 264 5701; fax: +81 54 264 5705.
E-mail address: oku@u-shizuoka-ken.ac.jp (N. Oku).

0304-3835/$ - see front matter © 2008 Elsevier Ireland Ltd. All rights reserved.
doi:10.1016/j.canlet.2008.05.009

fact, several drugs that inhibit VEGF signal transduction have been developed. For example, bevacizumab, a humanized anti-VEGF-A monoclonal antibody, and SU11248, a small molecule inhibitor against receptor tyrosine kinases (RTKs) of VEGF receptor (VEGFR) and platelet-derived growth factor receptor (PDGFR), have both been approved for cancer treatment [4].

Z-3-[(2,4-dimethylpyrrol-5-yl)methylidenyl]-2-indolinone (SU5416) is a potent inhibitor of VEGFR-2 tyrosine kinase [5]. The structure of SU5416 is shown in Fig. 1. This inhibitor has been shown to suppress VEGF-mediated angiogenesis in vitro and in vivo through the inhibition of autophosphorylation of VEGFR-2 by blocking the AMP-binding site within the kinase domain of the receptor [6]. It has been reported that SU5416 has no direct cytotoxic properties to cancer cells but inhibits tumor growth in numerous tumor xenograft models [7]. In Phase I and II trials, the therapeutic efficacy of SU5416 has been shown in combination with certain anticancer drugs. In a Phase III clinical trial, however, SU5416 showed no significant clinical benefit, and some patients showed striking responses induced by the toxicity of the solvent with Cremophor EL (CrEL) that was used to dissolve SU5416 for clinical administration [7–9]. Since CrEL has been known to induce various undesirable effects such as anaphylactic shock or hemolysis [10,11], coadministration with dexamethasone or other steroids is required to prevent hypersensitivity reactions [12]. Therefore, much effort has been devoted to improving the aqueous solubility of some agents to forgo using CrEL. For further enhancement of antiangiogenic effects and reduction of the side effects of SU5416, drug delivery systems (DDS) can be an important factor. However, studying antiangiogenic drugs in the field of DDS is not sufficient.

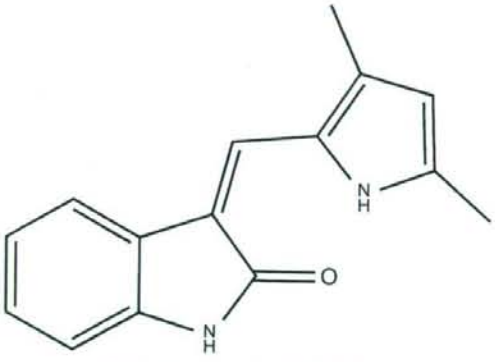

Molecular Formula: $C_{15}H_{14}N_2O$

Molecular Weight: 238.3

Fig. 1. Structure of 3-(3,5-dimethyl-1H-pyrrol-2-ylmethylene)-1, 3-dihydro-indol-2-one, SU5416.

Liposomes are small lipid vesicles and one of the most advanced drug nanocarriers in DDS studies [13]. As drug carriers, liposomes have various favorable characteristics for cancer therapy, such as low toxicity, long-term blood circulation, and accumulation in inflamed tissues and tumors by enhanced permeability and retention (EPR) effect [14,15]. Liposomal formulation of hydrophobic drugs has been shown to overcome the solubility problem and the solvent-induced side effect [16]. In addition, liposomes can be modified with various molecules, such as antibodies, carbohydrates, or peptides, to selectively target several kinds of cells [17]. In our previous studies, we identified angiogenic vessel-homing peptide Ala-Pro-Arg-Pro-Gly (APRPG), and utilized it in liposomal drug delivery. APRPG peptide-modified liposomes directly targeted angiogenic endothelial cells, and doxorubicin-incorporated APRPG-modified liposomes significantly suppressed tumor growth through the disruption of tumor neovasculature [18–20]. These studies raise the possibility that APRPG-modified liposomes are also useful drug carriers for targeted delivery of antiangiogenic drugs.

In this study, to overcome the solubility problem and to enhance the antiangiogenic effect of SU5416, we designed the SU5416-incorporated APRPG-modified liposome. We evaluated the characteristics of liposomal SU5416 as a liposomal drug, such as its encapsulation efficiency, stability in serum, VEGF inhibitory activity, and hemolytic activity in vitro. Subsequently, the therapeutic effect of APRPG-modified liposomal SU5416 in tumor-bearing mice was examined.

2. Materials and methods

2.1. Cell culture and materials

Colon26 NL-17 carcinoma cells were cultured in DMEM/Ham's F12 medium (WAKO, Osaka, Japan) supplemented with streptomycin (100 μg/ml), penicillin (100 U/ml), and 10% heat-inactivated fetal bovine serum (FBS, Japan Bio Serum Co., Ltd., Tokyo, Japan) at 37 °C in a 5% CO_2 atmosphere. Human umbilical vein

endothelial cells (HUVECs, Takara Bio Inc., Otsu, Shiga, Japan) were maintained in endothelial growth medium-2 (EGM-2, Cambrex Corporation, Walkersville, MD, USA) at 37 °C under 5% CO_2 in a humidified chamber. HUVECs used in this study were between passages 4 and 7. The lipids for preparing liposomes were the products of Nippon Fine Chemical, Co., Ltd., (Takasago, Hyogo, Japan).

2.2. Preparation of liposomal SU5416

Liposomes were prepared as described previously [19]. In brief, dipalmitoylphosphatidylcholine (DPPC), palmitoyl-oleoylphosphatidylcholine (POPC), cholesterol, and SU5416 solutions in chloroform were mixed (10:10:5:1 as a molar ratio) and dried under reduced pressure to make a thin lipid film. A distearoylphosphatidylethanolamine polyethyleneglycol (DSPE-PEG) or APRPG peptide-conjugated DSPE-PEG (DSPE-PEG-APRPG) solution was respectively, added to the initial lipid solutions in the proportion of 10-mol % to PC for the modification of the liposomes with PEG or PEG-APRPG. The thin lipid films were hydrated with 20 mM HEPES-buffered saline (pH 7.4), and the liposome solutions were frozen and thawed for three cycles with liquid nitrogen. The liposome size was then adjusted by extrusion through 100 nm-pore sized polycarbonate filters. The particle size and ζ-potential of liposomal SU5416 was measured using ZETASIZER (Malvern Instruments, Worcs, UK).

2.3. Determination of entrapment efficiency of SU5416 into liposomes

Liposomal SU5416 were prepared as described above. The prepared liposomes were fractionated by gel filtration chromatography using PD-10 column (GE Healthcare, UK. Ltd., Buckinghamshire, UK) according to the manufacturer's instruction. The turbidity of each fraction was determined by measuring the absorbance at 750 nm to define the liposome fractions. The amount of SU5416 in each fraction was quantified by absorption at 440 nm using high performance liquid chromatography (HPLC, HITACHI, Tokyo, Japan) equipped with ODS-80Ts column (Tosoh Corporation, Tokyo, Japan). The mobile phase for the HPLC analysis was composed of methanol and 35 mM KH_2PO_4 (3:1).

2.4. Stability of liposomal SU5416 in presence of serum

The prepared liposome solutions were incubated in the presence or absence of 50% FBS for 1 h at 37 °C. After that, the liposomes were separated by gel filtration chromatography using Sepharose™ 4 Fast Flow (Amersham Biosciences, Uppsala, Sweden) as described previously [21], and the amount of SU5416 in the liposome fractions was determined using HPLC as described above.

2.5. Cell proliferation assay

HUVECs were seeded (7500 cells/well) on a gelatin-coated 96-well plate and incubated overnight. After the change of medium to 0.5% FBS-containing endothelial basal medium-2 (EBM-2, Cambrex Corporation), the cells were treated with SU5416 (dissolved in DMSO), PEG-liposomal SU5416 (PEG-Lip-SU5416), or APRPG-PEG-liposomal SU5416 (APRPG-Lip-SU5416) and incubated for 3 h at 37 °C. Then, recombinant human $VEGF_{165}$ (20 ng/ml as final concentration, BD biosciences, San Diego, CA, USA) was added to the each well, and the cells were further incubated for 48 h. Colon26 NL-17 cells were seeded (3000 cells/well) on a 96-well plate in DMEM/Ham's F12 supplemented with 10% FBS and incubated overnight. Then, the cells were treated with the samples and further incubated for 48 h at 37 °C. The cell viability was measured with TetraColorOne™ (Seikagaku, Tokyo, Japan) according to the manufacturer's instruction.

2.6. Hemolytic assay

Free SU5416 was dissolved in the following components: polyethylene glycol 400; CrEL (Nakalai Tesque, Kyoto, Japan); benzyl alcohol; and dehydrated ethanol (45:31.5:2:21.5 w/w %) as described previously [7], and the SU5416 solution was diluted with 0.45% sodium chloride before treatment. Hemolytic assay was performed as described previously [22] with some modification. In brief, blood was obtained from 6-week-old BALB/c male mice (Japan SLC, Shizuoka, Japan). Red blood cells were collected by centrifugation (2000*g*, 5 min, 4 °C, five times) of the blood. The pellet was resuspended in 20 mM HEPES-buffered saline (pH 7.4) to give a 5% (v/v) solution. The suspension was added to HEPES-buffered saline, free SU5416, PEG-Lip-SU5416, or APRPG-Lip-SU5416 and incubated for 30, or 60 min at 37 °C. After centrifugation, the supernatants were transferred to a 96-well plate. Hemolytic activity was determined by measuring the absorption at 570 nm. Control samples of 0% lysis (in HEPES buffer) and 100% lysis (in 1% Triton X-100) were employed in the experiment.

2.7. Therapeutic experiment

Colon26 NL-17 carcinoma cells were subcutaneously implanted (1.0×10^6 cells) into the posterior flank of 4-week-old BALB/c male mice. HEPES-buffered saline (Control), free SU5416, PEG-Lip-SU5416, or APRPG-Lip-SU5416 was intravenously injected every other day (3 mg/kg/day as SU5416) from day 5 to day 13 after tumor implantation. The tumor size and body weight were monitored daily as described previously [19]. The animals were cared for according to the Guidelines for the Care and Use of Laboratory Animals of the University of Shizuoka.

2.8. Statistical analysis

Statistical analysis of the experiments was performed by unpaired Student's *t*-test using KaleidaGraph software (HULINKS, Tokyo, Japan).

3. Results

3.1. Characterization of liposomal SU5416

To investigate whether liposomal SU5416 has appropriate characteristics as a liposome agent, we examined its entrapment efficiency into the liposomes, particle size, ζ-potential, and its stability in the presence of serum. In gel filtration chromatography analysis, liposome fractions were defined by turbidity (absorption at 750 nm). More than 85% of SU5416 was detected in the liposome fractions of Control (non-modification), PEG- and APRPG-modified liposomes (Fig. 2). SU5416-encapsulated liposomes had approximately 130 nm of particle size and −3.0 mV of ζ-potential, respectively (Table 1). The notable change of particle size and the leakage of SU5416 from the liposomes were not observed until 14 days after preparation of the liposomes (Fig. 3). We also examined the stability of liposomal SU5416 in the presence of serum. PEG-Lip-SU5416 and APRPG-Lip-SU5416 were incubated with or without serum, and liposomal SU5416 was fractionated by gel filtration chromatography. After the incubation with serum, more than 85% of SU5416 in comparison with PBS alone were detected in the liposome fractions, fraction 5–10 (Fig. 4). These analyses revealed that SU5416 was effectively and stably encapsulated in the liposomes, and PEG-Lip- and APRPG-Lip-SU5416 stably existed in the presence of serum.

3.2. Growth inhibitory activity of liposomal SU5416

SU5416 has been shown to suppress endothelial cell proliferation through the inhibition of VEGF signal transduction [5]. To confirm that liposomal SU5416 has similar growth inhibitory activity against VEGF-stimulated endothelial cells, we performed a cell proliferation assay. PEG- and APRPG-Lip-SU5416 significantly inhibited endothelial cell proliferation induced by treatment with VEGF in a concentration dependent manner as well as free SU5416 (Fig. 5A). On the contrary, free SU5416 and liposomal SU5416 did not suppress the proliferation of Colon26 NL-17 carcinoma cells (Fig. 5B). These data suggest that encapsulated SU5416 maintains an inhibitory activity against VEGF signal transduction.

3.3. Suppression of hemolysis by liposomalization of SU5416

Since SU5416 is a hydrophobic compound, it is dissolved in the solvent containing CrEL for use in the

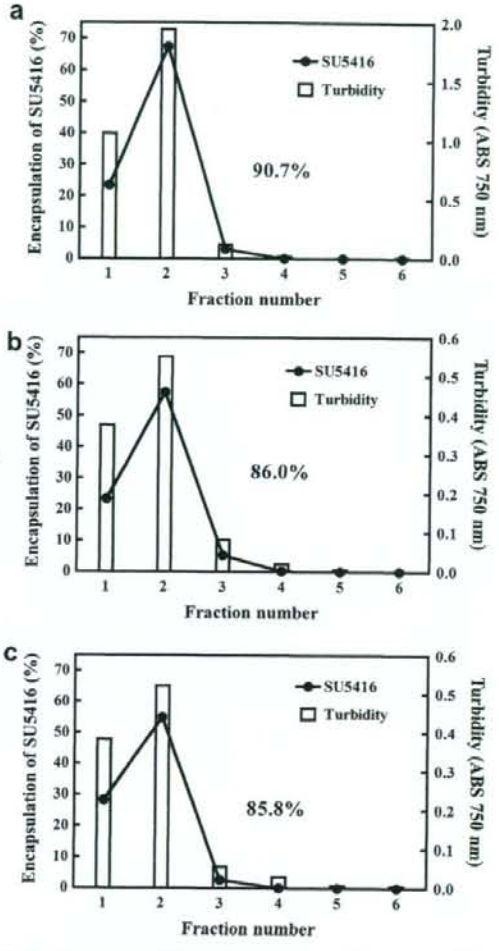

Fig. 2. Entrapment of SU5416 into Control, PEG- or APRPG-modified liposomes. Control liposomal SU5416 (a), PEG-modified liposomal SU5416 (b), and PEG-APRPG-modified liposomal SU5416 (c) were fractionated by gel filtration chromatography with PD-10 column. The turbidity (bar, left *Y* axis) was determined by measurement of the absorption at 750 nm, and the amount of SU5416 (dot, right *Y* axis) was measured using HPLC (absorption at 440 nm). The calculated entrapment efficiency is indicated in each graph.

Table 1
Particle size and ζ-potential of liposomal SU5416

	Particle size (nm)	ZP (mV)
PEG-Lip-SU5416	131.8 ± 14	−3.0 ± 2.2
APRPG-Lip-SU5416	142.6 ± 28	−3.0 ± 1.0

The data indicate the means ± SD.
ZP, ζ-potential.

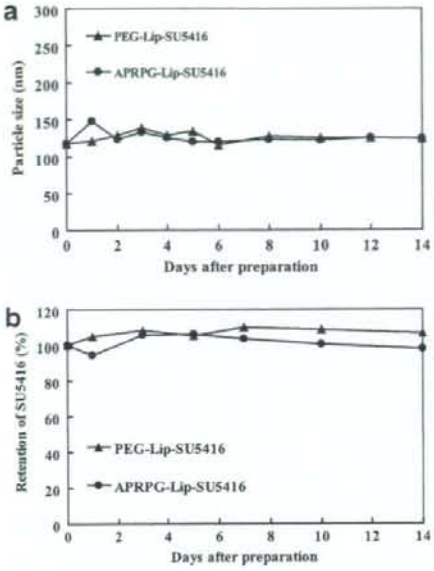

Fig. 3. Stability of liposomal SU5416 in particle size and entrapment efficiency. PEG- and APRPG-modified liposomal SU5416 were incubated until day 14 at 4 °C. The particle size of PEG-Lip-SU5416 (closed triangle) and APRPG-Lip-SU5416 (closed circle) was measured at indicated times (a). The amount of SU5416 into the liposomes was determined after gel filtration chromatography, and the relative entrapment efficiency was calculated as compared to that of the day 0 (b).

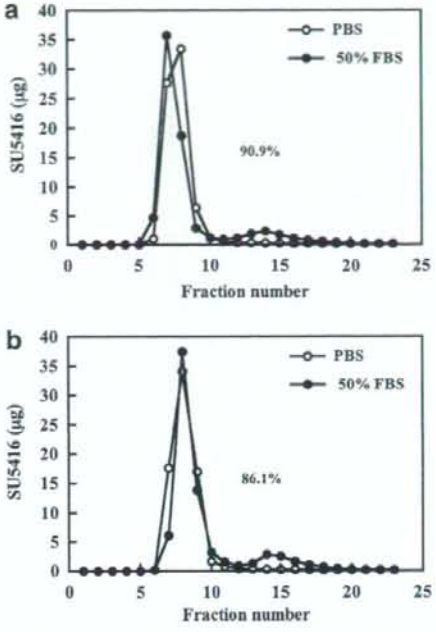

Fig. 4. Retention of SU5416 into liposomes in the presence of serum. PEG- (a) and APRPG-modified liposomal SU5416 (b) were incubated with (open circle) or without 50% fetal bovine serum (closed circle) for 1 h at 37 °C. Liposomal SU5416 was fractionated by gel filtration chromatography. The amount of SU5416 was measured using HPLC. The retention efficiency of SU5416 is indicated in each graph.

clinical studies. CrEL has been shown to induce some undesirable effects such as hemolysis [16]. To determine whether liposomalization of SU5416 precludes these side effects, we examined its hemolytic activity. Free SU5416 dissolved in the solvent induced remarkable hemolysis. In contrast, PEG- and APRPG-Lip-SU5416 showed a significantly low hemolytic activity (Fig. 6).

3.4. Tumor growth suppression by treatment with APRPG-modified liposomal SU5416 in tumor-bearing mice

Finally, the effect of APRPG-Lip-SU5416 in Colon26 NL-17 carcinoma cell-bearing mice was examined. APRPG-Lip-SU5416 significantly suppressed tumor growth compared with control ($p < 0.05$), free SU5416 ($p < 0.05$), and PEG-Lip-SU5416-treatment ($p < 0.01$, Fig. 7a). However, free SU5416 and PEG-Lip-SU5416 showed no tumor growth suppression under the present experimental conditions. SU5416- and liposomal SU5416-treatment did not affect the body weight changes of the mice, an indicator of a side effect (Fig. 7b). Although most of the mice showed shock-like behavior by injection intravenously with SU5416 dissolved in the CrEL-containing solvent, the behavior was not induced by liposomal SU5416 (data not shown).

4. Discussion

In this study, we attempted to develop neovasculature-targeted liposomal SU5416 to overcome the problem of solubility and to enhance the antiangiogenic activity of SU5416 through an active targeting strategy. Liposomal SU5416 has an appropriate particle size and an almost neutral electronic charge. These characteristics have been known to affect liposome distribution. In fact, it has been reported that liposomes having a particle size of approximately 100 nm and a neutral charge accumulate in inflammation region such as tumors through enhanced permeability and retention (EPR) effect [15]. It is also known that hydrophobic agents incorporated into the liposomal membrane transfer to plasma lipoproteins in the bloodstream. Therefore, we examined the stability of liposomal SU5416 in

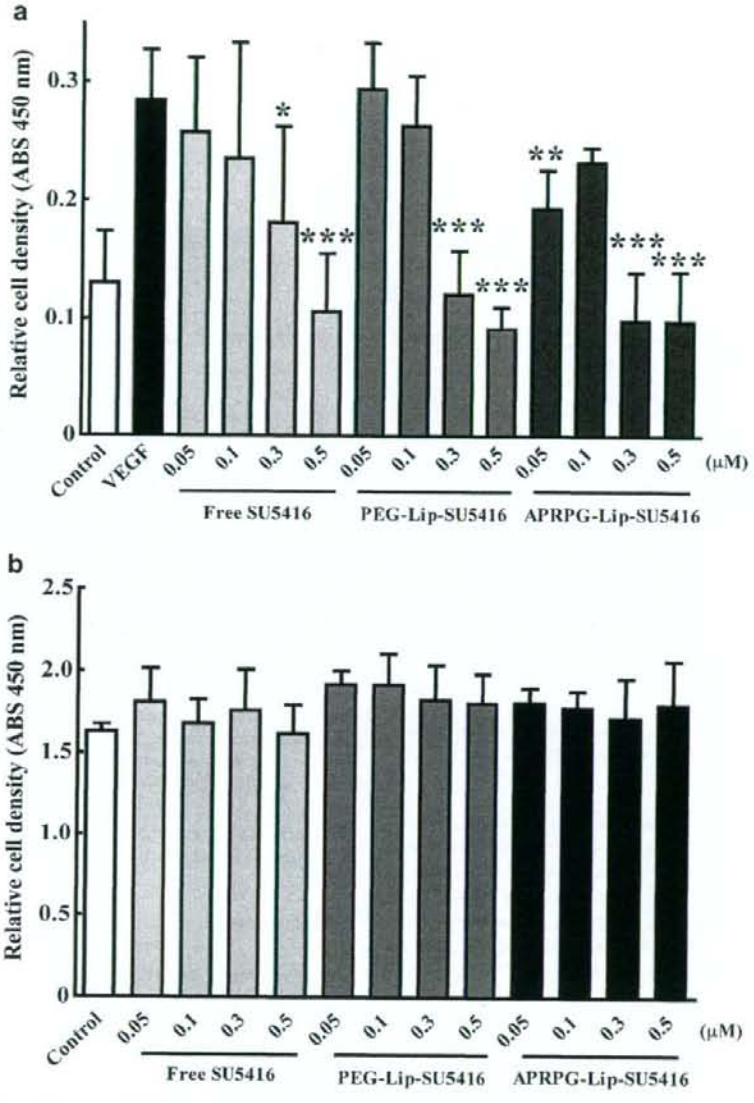

Fig. 5. Inhibited effect of liposomal SU5416 on VEGF-induced endothelial cell growth. (a) HUVECs (7500 cells/well) were seeded on a 96-well plate. The culture medium was changed to EBM-2 containing 0.5% FBS, and the cells were treated with free SU5416, PEG-Lip-SU5416, or APRPG-Lip-SU5416 at indicated concentration and incubated for 3 h at 37 °C. Then, the cells were added to $rhVEGF_{165}$ (20 ng/mL as final concentration) and further incubated for 48 h. (b) Colon26 NL-17 cells (3000 cells/well) were also seeded on a 96-well plate and incubated overnight. The cells were treated with these samples and further incubated for 48 h. Finally, cell viability was determined with TetraColor ONE™. The bars indicate the means ± SD. ($n = 4$), and the significant differences are indicated as follows: $^{*}p < 0.05$, $^{**}p < 0.01$, $^{***}p < 0.001$ versus VEGF-treated group.

the presence of serum, and observed it to be quite stable there. In addition, liposomalization of SU5416 maintained the antiangiogenic activity of SU5416. These findings suggest that SU5416-incorporated liposomes can adequately function as a liposomal drug.

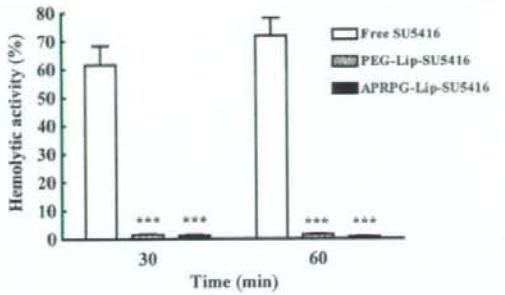

Fig. 6. Reduction of solvent-induced hemolysis by liposomalization of SU5416. Red blood cells were collected by centrifugation of the blood and resuspended in HEPES-buffered saline. The cell suspension was added to HEPES-buffered saline, free SU5416, PEG-Lip-SU5416, or APRPG-Lip-SU5416 and incubated for 30 or 60 min at 37 °C. After centrifugation, hemolytic activity was determined by measuring the absorbance (570 nm) of the supernatant. Control samples of 0% lysis (in HEPES buffer) and 100% lysis (in 1% Triton X-100) were employed in the experiment. The bars indicate the means ± SD. ($n = 4$). Significant difference is shown as follow: $^{***}p < 0.001$ versus free SU5416.

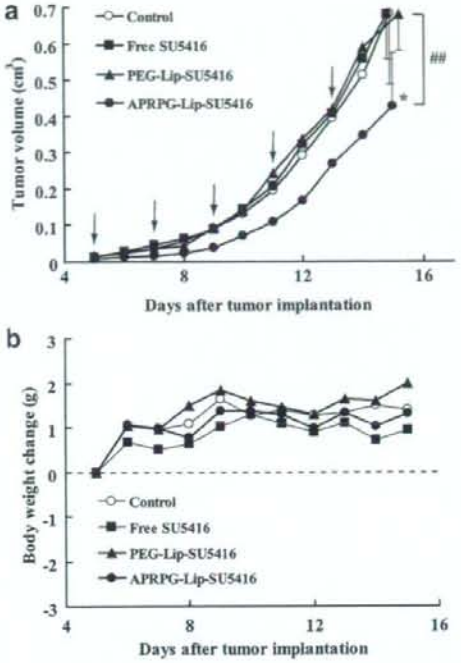

Fig. 7. Suppression of tumor growth by treatment with APRPG-modified liposomal SU5416 in tumor-bearing mice. Colon26 NL-17 carcinoma cells were implanted s.c. into the left posterior flank of 4-week-old BALB/c male mice ($n = 5$–6 per group). The mice were injected i.v. with HEPES buffer (Control, open circle), free SU5416 (3 mg/kg, closed square), PEG- (closed triangle) or APRPG-modified liposomal SU5416 (as SU5416 dosage, 3 mg/kg, closed circle) on days 5, 7, 9, 11, and 13 after tumor implantation. Tumor volume (a) and body weight change (b) were determined as described in the Section 2. Arrows show the days of injection. The data indicate the means ± SD, and the significant differences are indicated as follows: $^{*}p < 0.05$ versus control and free SU5416; $^{\#\#}p < 0.01$ versus PEG-Lip-SU5416.

We found that the liposomal SU5416 did not induce hemolysis in vitro and shock-like behaviors when it was intravenously injected. SU5416 is dissolved in the solvent containing CrEL that has been shown to induce various side effects [11]. Liposomes have also been used to formulate a variety of poorly water soluble drugs [23,24]. For example, by formulation into liposomes, paclitaxel, an anticancer drug used by dissolving in a mixture of 50% ethanol and 50% CrEL, has improved solubility, pharmacokinetics, and antitumor activity yet avoided any solvent-induced side effects [25,26]. Our findings suggest that liposomalization of SU5416 can overcome the solubility problem and decrease the risk of side effects caused by a solvent.

In an in vivo experiment, although APRPG-Lip-SU5416 did not exhibit any dramatic antitumor effect, it showed a statistically significant antitumor activity and without any prominent side effect. These results suggest that APRPG-modified liposomes may enhance antiangiogenic activity through targeted delivery of SU5416 to angiogenic endothelial cells in vivo. The previous study has shown that free SU5416 can suppress tumor growth by frequent injection at a high dose (10–25 mg/kg) [6], and therefore it is not thought to suppress tumor growth under the present treatment conditions (3 mg/kg/day, 5×). In addition, PEG-Lip-SU5416 also did not show the antitumor activity. One of the possible difference between APRPG-Lip-SU5416 and PEG-Lip-SU5416 is whether or not the liposomes directly target tumor endothelial cells [18,19]. PEG or other polymer modification is useful for a drug delivery system by the prolongation of drug circulation in the blood [27,28]. Since PEG liposomes accumulate in tumor tissues through the endothelial cell layer by the EPR effect, PEG-Lip-SU5416 seems to be weakly associated with angiogenic endothelial cells in the tumors. Our data suggest that active targeting to angiogenic endothelial cells may be an useful strategy to enhance the therapeutic effect of angiogenesis inhibitors. To improve the effect, it may be necessary to optimize liposome formulation (ligand

density, lipid composition, etc.) or to modify other ligands (antibodies, peptides, etc.).

In conclusion, we have shown that (i) SU5416 can be formulated in liposomes; (ii) Liposomal SU5416 can be administered without remarkable side effects; and (iii) APRPG-Lip-SU5416 exhibits higher antitumor activity than PEG-Lip-SU5416. Thus, tumor vasculature-targeted liposomes may be useful for drug delivery of antiangiogenic drugs, and the development of such DDS may advance antiangiogenic cancer therapy.

Acknowledgements

This research was supported by the Center of Excellence (COE) program in the 21st Century and Cooperation of Innovative Technology.

References

[1] P. Carmeliet, Angiogenesis in life, disease and medicine, Nature 438 (2005) 932–936.
[2] D. Neri, R. Bicknell, Tumour vascular targeting, Nat. Rev. Cancer 5 (2005) 436–446.
[3] N. Ferrara, H.P. Gerber, J. LeCouter, The biology of VEGF and its receptors, Nat. Med. 9 (2003) 669–676.
[4] W.A. Spannuth, A.K. Sood, R.L. Coleman, Angiogenesis as a strategic target for ovarian cancer therapy, Nat. Clin. Pract. Oncol. 5 (2008) 194–204.
[5] T.A. Fong, L.K. Shawver, L. Sun, C. Tang, H. App, T.J. Powell, Y.H. Kim, R. Schreck, X. Wang, W. Risau, A. Ullrich, K.P. Hirth, G. McMahon, SU5416 is a potent and selective inhibitor of the vascular endothelial growth factor receptor (Flk-1/KDR) that inhibits tyrosine kinase catalysis, tumor vascularization, and growth of multiple tumor types, Cancer Res. 59 (1999) 99–106.
[6] D.B. Mendel, R.E. Schreck, D.C. West, G. Li, L.M. Strawn, S.S. Tanciongco, S. Vasile, L.K. Shawver, J.M. Cherrington, The angiogenesis inhibitor SU5416 has long-lasting effects on vascular endothelial growth factor receptor phosphorylation and function, Clin. Cancer Res. 6 (2000) 4848–4858.
[7] M. Zangari, E. Anaissie, A. Stopeck, A. Morimoto, N. Tan, J. Lancet, M. Cooper, A. Hannah, G. Garcia-Manero, S. Faderl, H. Kantarjian, J. Cherrington, M. Albitar, F.J. Giles, Phase II study of SU5416, a small molecule vascular endothelial growth factor tyrosine kinase receptor inhibitor, in patients with refractory multiple myeloma, Clin. Cancer Res. 10 (2004) 88–95.
[8] A. Arora, E.M. Scholar, Role of tyrosine kinase inhibitors in cancer therapy, J. Pharmacol. Exp. Ther. 315 (2005) 971–979.
[9] C. Ye, D. Sweeny, J. Sukbuntherng, Q. Zhang, W. Tan, S. Wong, A. Madan, B. Ogilvie, A. Parkinson, L. Antonian, Distribution, metabolism, and excretion of the anti-angiogenic compound SU5416, Toxicol. In Vitro 20 (2006) 154–162.
[10] H. Gelderblom, J. Verweij, K. Nooter, A. Sparreboom, Cremophor EL: the drawbacks and advantages of vehicle selection for drug formulation, Eur. J. Cancer 37 (2001) 1590–1598.
[11] Y. Zou, H. Fu, S. Ghosh, D. Farquhar, J. Klostergaard, Antitumor activity of hydrophilic paclitaxel copolymer prodrug using locoregional delivery in human orthotopic non-small cell lung cancer xenograft models, Clin. Cancer Res. 10 (2004) 7382–7391.
[12] W.M. Stadler, D. Cao, N.J. Vogelzang, C.W. Ryan, K. Hoving, R. Wright, T. Karrison, E.E. Vokes, A randomized Phase II trial of the antiangiogenic agent SU5416 in hormone-refractory prostate cancer, Clin. Cancer Res. 10 (2004) 3365–3370.
[13] T.M. Allen, P.R. Cullis, Drug delivery systems: entering the mainstream, Science 303 (2004) 1818–1822.
[14] I. Cheong, X. Huang, K. Thornton, L.A. Diaz Jr., S. Zhou, Targeting cancer with bugs and liposomes: ready, aim, fire, Cancer Res. 67 (2007) 9605–9608.
[15] H. Maeda, J. Wu, T. Sawa, Y. Matsumura, K. Hori, Tumor vascular permeability and the EPR effect in macromolecular therapeutics: a review, J. Control. Release 65 (2000) 271–284.
[16] A.O. Nornoo, D.S. Chow, Cremophor-free intravenous microemulsions for paclitaxel II. Stability, in vitro release and pharmacokinetics, Int. J. Pharm. 349 (2008) 117–123.
[17] L. Nobs, F. Buchegger, R. Gurny, E. Allemann, Current methods for attaching targeting ligands to liposomes and nanoparticles, J. Pharm. Sci. 93 (2004) 1980–1992.
[18] N. Maeda, S. Miyazawa, K. Shimizu, T. Asai, S. Yonezawa, S. Kitazawa, Y. Namba, H. Tsukada, N. Oku, Enhancement of anticancer activity in antineovascular therapy is based on the intratumoral distribution of the active targeting carrier for anticancer drugs, Biol. Pharm. Bull. 29 (2006) 1936–1940.
[19] N. Maeda, Y. Takeuchi, M. Takada, Y. Sadzuka, Y. Namba, N. Oku, Anti-neovascular therapy by use of tumor neovasculature-targeted long-circulating liposome, J. Control. Release 100 (2004) 41–52.
[20] N. Oku, T. Asai, K. Watanabe, K. Kuromi, M. Nagatsuka, K. Kurohane, H. Kikkawa, K. Ogino, M. Tanaka, D. Ishikawa, H. Tsukada, M. Momose, J. Nakayama, T. Taki, Anti-neovascular therapy using novel peptides homing to angiogenic vessels, Oncogene 21 (2002) 2662–2669.
[21] K. Ichikawa, T. Urakami, S. Yonezawa, H. Miyauchi, K. Shimizu, T. Asai, N. Oku, Enhanced desensitization efficacy by liposomal conjugation of a specific antigen, Int. J. Pharm. 336 (2007) 391–395.
[22] D. Guggi, N. Langoth, M.H. Hoffer, M. Wirth, A. Bernkop-Schnurch, Comparative evaluation of cytotoxicity of a glucosamine-TBA conjugate and a chitosan-TBA conjugate, Int. J. Pharm. 278 (2004) 353–360.
[23] P. Crosasso, M. Ceruti, P. Brusa, S. Arpicco, F. Dosio, L. Cattel, Preparation characterization and properties of sterically stabilized paclitaxel-containing liposomes, J. Control. Release 63 (2000) 19–30.
[24] S. Kim, Liposomes as carriers of cancer chemotherapy, current status and future prospects, Drugs 46 (1993) 618–638.
[25] A. Sharma, E. Mayhew, L. Bolcsak, C. Cavanaugh, P. Harmon, A. Janoff, R.J. Bernacki, Activity of paclitaxel liposome formulations against human ovarian tumor xenografts, Int. J. Cancer 71 (1997) 103–107.
[26] T. Yang, F.D. Cui, M.K. Choi, J.W. Cho, S.J. Chung, C.K. Shim, D.D. Kim, Enhanced solubility and stability of

PEGylated liposomal paclitaxel: in vitro and in vivo evaluation, Int. J. Pharm. 338 (2007) 317–326.
[27] R. Satchi-Fainaro, M. Puder, J.W. Davies, H.T. Tran, D.A. Sampson, A.K. Greene, G. Corfas, J. Folkman, Targeting angiogenesis with a conjugate of HPMA copolymer and TNP-470, Nat. Med. 10 (2004) 255–261.
[28] M.J. Vicent, R. Duncan, Polymer conjugates: nanosized medicines for treating cancer, Trends Biotechnol. 24 (2006) 39–47.

Identification of prognostic biomarkers in gastric cancer using endoscopic biopsy samples

Yasuhide Yamada,[1] Tokuzo Arao,[2] Takuji Gotoda,[3] Hirokazu Taniguchi,[4] Ichiro Oda,[3] Kuniaki Shirao,[1] Yasuhiro Shimada,[1] Tetsuya Hamaguchi,[1] Ken Kato,[1] Tetsutaro Hamano,[7] Fumiaki Koizumi,[5] Tomohide Tamura,[1] Daizo Saito,[3] Tadakazu Shimoda,[4] Makoto Saka,[6] Takeo Fukagawa,[6] Hitoshi Katai,[6] Takeshi Sano,[6] Mitsuru Sasako[6] and Kazuto Nishio[2,8]

[1]Medical Oncology, [3]Endoscopic Division, [4]Diagnostic Pathology Division, [5]Shien Lab, and [6]Surgical Division, National Cancer Center Hospital, 5-1-1 Tsukiji, Chuo-ku, Tokyo 104-0045; [2]Department of Genome Biology, Kinki University School of Medicine, 377-2 Ohno-Higashi, Osaka-Sayama, Osaka 589-8511; [7]Hamano Statistical Analysis Ltd, 6-7-15 Chuo-cho, Higashikurume, Tokyo 203-0054, Japan

(Received June 22, 2008/Revised July 16, 2008/Accepted July 16, 2008/Online publication September 28, 2008)

Endoscopic biopsy prior to chemotherapy provides an opportunity for studying biomarkers to predict the overall survival in gastric cancer patients. This prospective study was performed to identify prognostic biomarkers in patients with unresected gastric cancer. Fifty-nine cases of chemotherapy-naive metastatic gastric cancer were enrolled in this study. A microarray analysis was performed using 40 biopsy samples to identify candidate genes whose expressions might be correlated with the overall survival. After adjusting for clinical covariates based on a multivariate analysis, the identified genes were validated using real-time reverse transcription polymerase chain reaction (RT-PCR) analysis in 19 independent validation samples. Ninety-eight candidate genes whose expression levels were significantly correlated with the overall survival were identified using a microarray analysis based on a proportional hazards model ($P < 0.005$). Multivariate analysis was performed to assess 10 of these genes, and the results yielded a statistical significance level for *DACH1* and *PDCD6*. We further evaluated these two genes in independent samples using real-time RT-PCR and found that lower mRNA expression levels of *PDCD6* were correlated significantly with a poor overall survival. We identified *PDCD6* as a prognostic biomarker in patients with unresected gastric cancer using endoscopic biopsy samples. Our PCR-based single gene prediction strategy successfully predicted the overall survival and may lead to a better understanding of this disease subgroup. (*Cancer Sci* 2008; 99: 2193–2199)

Over the past two decades, various anticancer agents have been examined for their efficacy against gastric cancer, including 5-fluorouracil (5-FU) and 5-FU-based drugs, taxanes, CPT-11 and cisplatin, all administered either as monotherapy or in combination regimens;[1] however, the median survival time (MST) of these patients remains at only approximately 7 months.[2,3] In a recent randomized phase III trial examining oral S-1 monotherapy and cisplatin plus irinotecan combination therapy, the response rates to both S-1 and to the cisplatin plus irinotecan combination therapy were approximately 50%, indicating that around half of the patients did not respond to chemotherapy,[4–7] and the MST in both the arms was less than 1 year.[8] Thus, the prognosis of patients with gastric cancer remains poor.

The commonly recognized prognostic factors in cases of unresectable gastric cancer are the performance status, presence/absence of liver metastases, presence/absence of peritoneal metastases and the serum levels of alkaline phosphatase.[9] Many molecular biomarkers have been also investigated for their potential to predict the outcome in hypothesis-based studies. Several studies have shown that the mRNA levels and immunohistochemical staining intensity of thymidylate synthase (TS) in gastric cancers treated with fluorouracil are associated with the response and survival; in addition, the excision repair cross-complementing (ERCC)1 gene expression level has been shown to be associated with the clinical outcome in patients treated with cisplatin.[10,11] HER2 expression has also been reported to be a prognostic marker in cases of differentiated gastric cancer.[12,13] Mutation of p53 and high p53 protein expression, and high expression levels of urokinase-plasminogen activator, xanthine oxidoreductase, claudin-4, vascular endothelial growth factor, interleukin-8 and cyclin E have all been correlated with poor survival.[13–19] In terms of epigenetic alterations, reduced expression of acetylated histone H4 or DNA methylation of CDH1 and RAR-β have been shown to be correlated with tumor invasiveness and the tumor metastasizing potential.[20,21]

On the other hand, the recent introduction of the microarray technology has enabled significant genes to be identified almost throughout the genome using a hypothesis-free approach. The possibility of performing genome-wide searches is a major advantage, and such searches may be the only way to discover genes that would otherwise be unlikely to even be suggested as candidates. In gastric cancer, biopsy samples of the primary lesions can be easily obtained by endoscopy prior to treatment; however, few prospective biomarker studies using endoscopic biopsy samples to predict patient outcome have been performed to date. Therefore, we conducted a prospective study to identify biomarkers for predicting survival in patients with unresected metastatic gastric cancer.

Materials and Methods

Patients and samples. The eligible subjects in this study were patients with histologically confirmed, untreated and metastatic stage IV gastric cancer between 20 and 75 years of age. Additional inclusion criteria included an Eastern Cooperative Oncology Group performance status of 0–2. The exclusion criteria included history of prior chemotherapy or major surgery. All patients received chemotherapy using a 5-FU-based regimen (5-FU alone, S1 alone, 5-FU + methotrexate, 5-FU + cisplatin, or S1 + cisplatin) or a CPT-11 plus cisplatin regimen. Sixty-five gastric cancer patients were enrolled in the study. Of these, two were excluded because of insufficient RNA quantities extracted from their biopsy specimens, and four were excluded because of the poor RNA quality. Thus, samples from the remaining 59 patients were analyzed. The survival time was followed after the patients were initiated on chemotherapy. This study was approved

[8]To whom correspondence should be addressed. E-mail: knishio@med.kindai.ac.jp

doi: 10.1111/j.1349-7006.2008.00935.x

by the Institutional Review Board of the National Cancer Center Hospital, and written informed consent was obtained from all the patients.

The endoscopic biopsy samples collected were immediately placed in an RNA stabilization solution (Isogen; Nippongene, Tokyo, Japan) and stored at –80°C. Other biopsy samples obtained from the same location were reviewed by a pathologist to confirm the presence of tumor cells. The RNA extraction method and the quality check protocol have been described previously.[22]

Study design. This prospective study was started in July 2003 and enrollment was completed in November 2006 at the National Cancer Center Hospital. Fifty-nine gastric cancer samples were evaluated in this study. The samples were divided into a training set ($n = 40$) and a validation set ($n = 19$; 2:1) using computer-generated randomization (Microsoft Office Excel, Microsoft, Redmond, WA, USA). A microarray analysis was performed using the training set of 40 samples, and candidate genes whose expressions were correlated with the overall survival were identified. Multivariate analysis was performed to adjust the expression of 10 of these candidate genes for clinical features. Finally, the significant genes were evaluated in an independent set of 19 samples and survival was predicted using the results of real-time reverse transcription polymerase chain reaction (RT-PCR) analyses.

Real-time RT-PCR. Real-time RT-PCR was performed for 10 genes: *DACH1* (dachshund homolog 1, NM_004392); *EGFR* (epidermal growth factor receptor, NM_005228); *MT1X* (metallothionein 1X, NM_005952); *YWHAE* (tyrosine 3-monooxygenase/tryptophan 5-monooxygenase activation protein, epsilon polypeptide, NM_006761); *GPX3* (glutathione peroxidase 3, NM_002084); *PDCD6* (programmed cell death 6, NM_013232); *WDR33* (WD repeat domain 33, NM_018383); *C14orf43* (chromosome 14 open reading frame 43, NM_194278); *MYLIP* (myosin regulatory light chain interacting protein, NM_013262); and *GKAP1* (G kinase anchoring protein 1, NM_025211). Glyceraldehyde 3 phosphate dehydrogenase (*GAPD*, NM_002046) was used to normalize the expression levels in the subsequent quantitative analyses. RNA was converted to cDNA using a GeneAmp RNA PCR Core kit (Applied Biosystems, Foster City, CA). The transcripts were quantified using the Power SYBR Green PCR Master Mix (Applied Biosystems) and 7900HT Fast Real-time PCR system (Applied Biosystems) and reported relative to the *GAPD* expression levels. The PCR conditions were as follows: one cycle of denaturation at 95°C for 10 min, followed by 40 cycles at 95°C for 15 s and 60°C for 60 s. To amplify the target genes, the following primers were purchased from Takara (Yotsukaichi, Japan): DACH1-FW, 5′-AAG GGC TGC TAA AGC AAT CAG G-3′, and DACH1-RW, 5′-CTT TGT GGC AAA GCG ACA TTA GG-3′; EGFR-FW, 5′-GGT GCG AAT GAC AGT AGC ATT ATG A-3′, and EGFR-RW, 5′-AAA TGG GCT CCT AAC TAG CTG AAT C-3′; MT1X-FW, 5′-TTG ATC GGG AAC TCC TGC TTC T-3′, and MT1X-RW, 5′-ACA CTT GGC ACA GCC GAC A-3′; GPX3-FW, 5′-ATG CCT ACA GGT ATG CGT GAT TG-3′, and GPX3-RW, 5′-TGC AGG CAC ACA GAT GGT ACA-3′; PDCD6-FW, 5′-TCA AGG CCA GAC TAG ATC AGC CTA A-3′, and PDCD6-RW, 5′-GCT GGG ATG AGG CAC ATG AC-3′; YWHAE-FW, 5′-GGC AGA ATT TGC CAC AGG AA-3′, and YWHAE-RW, 5′-ACC TAA GCG AAT AGG ATG CGT TG-3′; WDR33-FW, 5′-ATG CAT GGG CTC TGT CAG TTT C-3′, and WDR33-RW, 5′-GGC TGA TAC CGG GAC AAC ACT AC-3′; C14orf43-FW, 5′-CAG ACT GGC AAG CCT AAC TCC ATA-3′, and C14orf43-RW, 5′-CAA GGC TGT TCC TGT GCT CTG-3′; MYLIP-FW, 5′-ACG TCT ATC TGC CAA CGC ACA C-3′, and MYLIP-RW, 5′-CAG TTC ATG GAA ACA TGC CAA GTC-3′; GKAP1-FW, 5′-TTG CGA ATA AGT TTC GGA GCA TC-3′, and GKAP1-RW, 5′-GCC ACT GCC ACT ATC CAC TTG TAA-3′; GAPD-FW, 5′-GCA CCG TCA AGG CTG AGA AC-3′, and GAPD-RW, 5′-ATG GTG GTG AAG ACG CCA GT-3′.

Oligonucleotide microarray study. The microarray procedure was performed according to the Affymetrix protocols (Santa Clara, CA). In brief, the total RNA extracted from the tumor samples was analyzed using an Agilent 2100 Bioanalyzer (Agilent Technologies, Waldbronn, Germany) for quality check, and cRNA was synthesized using the GeneChip 3′-Amplification Reagents One-Cycle cDNA Synthesis Kit (Affymetrix). The labeled cRNA were then purified and used for construction of the probes. Hybridization was performed using the Affymetrix GeneChip HG-U133 Plus 2.0 array for 16 h at 45°C. The signal intensities were measured using a GeneChip Scanner3000 (Affymetrix) and converted to numerical data using the GeneChip Operating Software, ver. 1 (Affymetrix).

Statistical analysis. The microarray analysis was performed using the BRB Array Tools software ver. 3.3.0 (http://linus.nci.nih.gov/BRB-ArrayTools.html) developed by Dr Richard Simon and Dr Amy Peng. In brief, a log base 2 transformation was applied to the raw microarray data, and global normalization was used to calculate the median over the entire array. Genes were excluded if the percentage of data missing or filtered out exceeded 20%. Genes that passed the filtering criteria were then considered for further analysis. We computed a statistical significance level ($P < 0.005$) for each gene based on a univariate proportional hazards model.

To adjust the expression of 10 genes (*DACH1*, *EGFR*, *MT1X*, *YWHAE*, *GPX3*, *PDCD6*, *WDR33*, *C14orf43*, *MYLIP* and *GKAP1*) for clinical features (age, sex, performance status [PS], number of metastatic sites, received chemotherapy), clinical data and the normalized microarray expression data of the 10 genes were imported into SAS software ver. 9.1.3 (SAS Institute, Cary, NC, USA) and a Cox regression model was constructed for multivariate analysis against each of the variables. The study groups were divided into two groups based on each of the clinical features: age (<65 or ≥65 years), sex (male or female), PS (0 or ≥1), number of metastatic sites (<3 or ≥3), chemotherapy (5-FU-based or CPT11 + CDDP) and expression levels of 10 genes). $P < 0.05$ was considered significant.

Results

Identification of 98 candidate prognosis-related genes using a microarray analysis. The univariate analysis of clinical features including age (<65 or ≥65 years), sex, PS (0 or ≥1), number of metastatic sites (1, 2 or ≥3) and received chemotherapy (5-FU-based or CPT11 + CDDP) were performed for 40 microarray samples (Table 1). There were no significant differences between any of the two groups divided according to age, sex, number of metastatic sites or received chemotherapy; however, significant differences were noted between the two groups divided according to PS ($P = 0.048$).

To identify the candidate prognosis-related genes from amongst over 47 000 transcripts, a microarray analysis was performed for a training set of 40 samples. A total of 21 308 genes passed the filtering criteria and were further analyzed. Ninety-eight genes were significantly correlated with survival, according to a Cox proportional hazards model ($P < 0.005$) (Table 2). Fifty-nine genes were protective genes (hazard ratio, <1), and 39 were risk genes (hazard ratio >1).

A heat-map of the expression values of the 98 selected genes comparing the unfavorable prognosis group (survival time, <180 days) and favorable prognosis group (survival time, ≥180 days) is shown in Fig. 1. Genes are plotted via hierarchical clustering.

Multivariate analysis of prognosis-related genes. Of the 98 candidate genes, we prioritized those that: (i) were selected by overlapping probes; (ii) were novel genes; or (iii) had a lower

doi: 10.1111/j.1349-7006.2008.00935.x

Table 1. Univariate analysis of clinical features

Variable	No. of patients	MST (days)	*P*-value (log-rank test)
Age (years)			
≥65	16	235	0.454
<65	24	250	
Sex			
Male	29	243	0.926
Female	11	267	
PS			
≥1	24	182	0.048
0	16	309	
Metastasis			
1, 2	10	137	0.102
≥3	30	261	
Chemotherapy			
5-FU-based	26	245	0.594
CPT11 + CDDP	14	240	

MST, median survival time; PS, performance status.

P-value according to a Cox proportional hazards model. We selected the following 10 genes of interest for real-time RT-PCR analysis: *DACH1*, *EGFR*, *MT1X*, *YWHAE*, *GPX3*, *PDCD6*, *WDR33*, *C14orf43*, *MYLIP* and *GKAP1*.

To adjust for relevant clinical covariates against these 10 genes, we performed a multivariate analysis (Table 3). The results of the multivariate analysis revealed that high *DACH1* expression and high *PDCD6* expression were significantly correlated with the favorable outcome ($P = 0.0134$ and $P = 0.0015$, respectively). We therefore considered that the *DACH1* and *PDCD6* expressions were independent prognostic markers from the results of the multivariate analysis. Results of microarray data and patient survival in the training set of 40 patients are shown in Fig. 2. The Kaplan–Meier method was used for *DACH1* and *PDCD6*. The low *PDCD6* and *DACH1* expression groups had significantly poorer outcomes ($P < 0.0001$ and $P = 0.0045$).

Validation using real-time RT-PCR in independent samples. The mRNA expression levels of *DACH1* and *PDCD6* were quantified using real-time RT-PCR in 19 independent samples to validate the results of the microarray. While the expression levels of *DACH1* were not correlated with survival, those of *PDCD6* in independent samples were significantly correlated with the survival ($P = 0.007$) (Table 4). The Kaplan–Meier method was used to estimate the overall survival using the median value (Fig. 3a). All quantified expression levels of real time RT-PCR data are shown as Fig. 3(b). The mRNA expressions of *PDCD6* varied by approximately 25 fold (range, 0.98–25.1). The low *PDCD6* expression groups had significantly poorer outcomes ($P = 0.0018$). We concluded that *PDCD6* was a valuable gene for predicting the survival in patients with gastric cancer. These results indicate that our PCR-based single gene prediction strategy using endoscopic biopsy samples could successfully predict the overall patient survival.

Discussion

Several studies have identified prognostic biomarkers in cases of gastric cancer using microarray analysis. Hasegawa *et al.* identified 12 genes that were associated with lymph node metastasis.[23] Hippo *et al.* identified several genes associated with lymph node metastasis, including Oct-2, and genes associated with the histological type, including liver-intestine cadherin.[24] These studies introduced a novel direction in which microarray analysis could be used to predict postoperative recurrences. Inoue *et al.* selected 78 genes that were differentially expressed between aggressive and non-aggressive cancers and constructed a prognostic scoring system.[25] Leung *et al.* found that high CCL18 expression levels were associated with prolonged overall and disease-free survival.[26] They also found that phospholipase A2 group IIA expression in gastric adenocarcinoma was associated with prolonged survival and less frequent metastasis.[27] Chen *et al.* demonstrated a survival prediction model consisting of three genes (*CD36*, *SLAM*, *PIM-1*) that was capable of predicting poor or good survival in 23 (76.7%) of 30 newly enrolled patients.[28] Most of these studies used surgical specimens to predict postsurgical survival and were conducted retrospectively. Thus, we think that our present prospective study is unique in that we used endoscopic biopsy samples to predict the survival time in patients with unresectable gastric cancer. In patients with unresectable cancer, endoscopic biopsy samples may be the most appropriate specimens available non-invasively for microarray analysis. Although tumor heterogeneity may pose problems when biopsy samples are used as representative tissue specimens and further investigation is required, we believe that endoscopic biopsy samples should continue to be used for microarray analyses. Current clinical study has been confronted with a number of obstacles. Microarray analysis for clinical studies, in particular, has been hampered with bottlenecks such as RNA quality, the extremely large number of genes to be analyzed, an immature analytical tool or methodology and so on. There are two types of obstacles: controllable obstacles and uncontrollable ones. One uncontrollable obstacle is a complex chemotherapy regimen. It is easy to say that a clinical biomarker study should be performed in one particular regimen. Chemotherapy regimen has, however, progressed and become more sophisticated in a short range of time. This study was prospective clinical study and was largely followed by a guideline, Recommendations for Tumor Marker Prognostic Studies (REMARK). To minimize

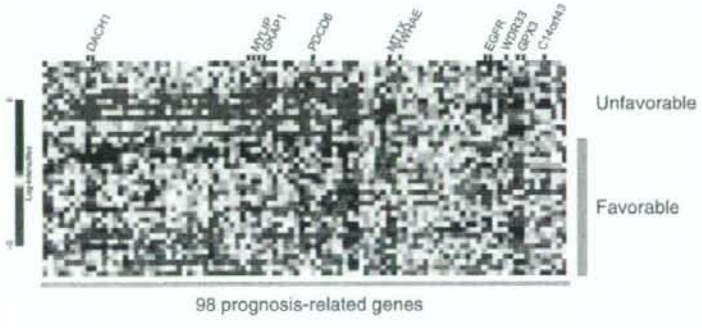

Fig. 1. Heat map of expression values for microarray identifying 98 genes whose expressions were correlated with survival. The hierarchical clustering of the 98 genes comparing the unfavorable prognosis group (survival time, <180 days) and favorable prognosis group (survival time, ≥180 days) is shown. The blue or red colors of each block represent the normalized gene expression levels. Each row represents a sample, and each column represents a gene. The 10 genes included in the multivariate analysis (Table 3) are shown.

Table 2. Prognosis-related genes identified using microarray analysis

P-value	Hazard ratio	Description	Gene	Probe set	Pass	PCR		
0.0002	1.8	Epidermal growth factor receptor	*EGFR*	201984_s_at	2	PCR	1	0.1
0.0005	0.1	DEAD (Asp-Glu-Ala-Asp) box polypeptide 54	*DDX54*	219111_s_at			2	0.1
0.0005	0.5	Chimerin (chimaerin) 2	*CHN2*	213385_at			3	0.1
0.0005	6.1	Ubiquitin-like domain containing CTD phosphatase 1	*UBLCP1*	227413_at			4	0.2
0.0006	0.5	PTK2 protein tyrosine kinase 2	*PTK2*	241387_at			5	0.2
0.0008	3.4	Der1-like domain family, member 2	*DERL2*	218333_at			6	0.2
0.0008	0.5	Leucine rich repeat containing 14	*LRRC14*	32062_at			7	0.2
0.0009	4.5	WD repeat domain 33	*WDR33*	222763_s_at		PCR	8	0.2
0.0009	0.1	Rhomboid domain containing 3	*RHBDD3*	217622_at			9	0.2
0.001	0.3	Myosin regulatory light chain interacting protein	*MYLIP*	228098_s_at	3	PCR	10	0.2
0.0013	4.7	Chromosome 14 open reading frame 43	*C14orf43*	225980_at		PCR	11	0.2
0.0013	0.2	BCL6 co-repressor	*BCOR*	223915_at			12	0.2
0.0013	0.5	MAD1 mitotic arrest deficient-like 1 (yeast)	*MAD1L1*	233921_s_at			13	0.2
0.0013	4.9	Chromosome 14 open reading frame 109	*C14orf109*	213246_at			14	0.2
0.0014	4.2	Hypothetical protein LOC124512	*LOC124512*	225808_at			15	0.2
0.0014	5.0	Ring finger protein 167	*RNF167*	212047_s_at			16	0.2
0.0014	0.6	Hypothetical LOC25845	*LOC25845*	225457_s_at			17	0.2
0.0014	4.2	General transcription factor II, i	*GTF2I*	232710_at			18	0.3
0.0014	0.2	Rho guanine nucleotide exchange factor (GEF) 10-like	*ARHGEF10L*	1570511_at			19	0.3
0.0014	0.3	G kinase anchoring protein 1	*GKAP1*	229312_s_at		PCR	20	0.3
0.0015	1.9	Glutathione peroxidase 3 (plasma)	*GPX3*	214091_s_at	2	PCR	21	0.3
0.0016	0.5	Dachshund homolog 1 (*Drosophila*)	*DACH1*	1567101_at	2	PCR	22	0.3
0.0016	0.3	Diacylglycerol kinase, theta 110kDa	*DGKQ*	226605_at			23	0.3
0.0017	0.6	Hepatocellular carcinoma-associated antigen 112	*HCA112*	218345_at			24	0.3
0.0018	3.5	Mediator of RNA polymerase II transcription, subunit 31 homolog	*MED31*	222867_s_at			25	0.3
0.0018	6.9	Tyrosine 3-monooxygenase/tryptophan 5-monooxygenase activation protein, epsilon polypeptide	*YWHAE*	210317_s_at		PCR	26	0.3
0.0018	0.1	KH domain containing, RNA binding, signal transduction associated 1	*KHDRBS1*	201488_x_at			27	0.3
0.0019	0.3	Solute carrier family 25 (mitochondrial carrier; Graves disease autoantigen), member 16	*SLC25A16*	210686_x_at			28	0.3
0.0019	4.9	Hypothetical protein LOC51255	*LOC51255*	223064_at			29	0.3
0.002	0.2	Cyclin L2 /// similar to Aurora kinase A-interacting protein	*CCNL2 /// LOC643556*	222999_s_at			30	0.3
0.002	7.4	Lectin, mannose-binding, 1	*LMAN1*	224629_at			31	0.3
0.002	0.2	Erythrocyte membrane protein band 4.1 like 4A	*EPB41L4A*	228259_s_at			32	0.3
0.0022	0.2	KIAA0999 protein	*KIAA0999*	204155_s_at			33	0.3
0.0022	0.5	ELOVL family member 7	*ELOVL7*	227180_at			34	0.3
0.0023	4.0	Churchill domain containing 1	*CHURC1*	233268_s_at			35	0.4
0.0024	4.0	Yippee-like 2 (*Drosophila*)	*YPEL2*	227020_at			36	0.4
0.0024	5.9	Hermansky–Pudlak syndrome 1	*HPS1*	210112_at			37	0.4
0.0025	0.3	Hypothetical protein LOC285831	*LOC285831*	228857_at			38	0.4
0.0026	3.5	CDC37 cell division cycle 37 homolog (*Saccharomyces cerevisiae*)-like 1	*CDC37L1*	219343_at			39	0.4
0.0026	2.1	Ankyrin repeat and SOCS box-containing 9	*ASB9*	205673_s_at			40	0.4
0.0026	0.2	Hypothetical gene supported by AK125149	*LOC401577*	239247_at			41	0.5
0.0026	0.3	TBC1 domain family, member 23	*TBC1D23*	236755_at			42	0.5
0.0026	0.3	MRNA full length insert cDNA clone EUROIMAGE 2362292		235505_s_at			43	0.5
0.0026	0.4	Dehydrogenase/reductase (SDR family) member 8	*DHRS8*	217989_at			44	0.5
0.0026	0.4	Nuclear receptor coactivator 2	*NCOA2*	242369_x_at			45	0.5
0.0026	0.2	MRNA; cDNA DKFZp667E0114 (from clone DKFZp667E0114)		235660_at			46	0.5
0.0027	0.4	Transforming, acidic coiled-coil containing protein 1	*TACC1*	242290_at			47	0.5
0.0027	0.2	POU domain, class 2, transcription factor 1	*POU2F1*	1562280_at			48	0.5
0.0027	2.9	p21(CDKN1A)-activated kinase 6	*PAK6*	1555310_a_at				0.5
0.0027	0.5	Mannosyl (alpha-1,3-)-glycoprotein β-1,4-N-acetylglucosaminyltransferase, isozyme A	*MGAT4A*	226039_at			50	0.5
0.0027	5.1	Zinc finger CCCH-type containing 14	*ZC3H14*	204216_s_at			51	0.5
0.0028	0.5	Acyl-CoA synthetase short-chain family member 2	*ACSS2*	235805_at			52	0.5
0.0028	0.3	Programmed cell death 6	*PDCD6*	222380_s_at		PCR	53	0.6
0.0029	3.8	ERGIC and golgi 2	*ERGIC2*	226422_at			54	0.6
0.0029	0.4	Erythrocyte membrane protein band 4.1 like 5	*EPB41L5*	225855_at			55	0.6
0.003	6.5	Chromosome 14 open reading frame 32	*C14orf32*	212644_s_at			56	0.6

doi: 10.1111/j.1349-7006.2008.00935.x

Table 2. (*Continued*)

P-value	Hazard ratio	Description	Gene	Probe set	Pass	PCR		
0.0031	0.2	Transcribed locus		239437_at			57	1.8
0.0031	0.3	DOT1-like, histone H3 methyltransferase (*S. cerevisiae*)	*DOT1L*	231297_at			58	1.9
0.0031	2.2	Transcription elongation factor A (SII)-like 8	*TCEAL8*	224819_at			59	1.9
0.0031	0.3	Laminin, β 1	*LAMB1*	236437_at			60	2.0
0.0032	2.7	FK506 binding protein 5	*FKBP5*	224840_at			61	2.0
0.0033	0.5	Integrin, α 6	*ITGA6*	244665_at			62	2.1
0.0034	2.7	COMM domain containing 9	*COMMD9*	218072_at			63	2.2
0.0034	0.2	Eukaryotic translation initiation factor 4 γ, 3	*EIF4G3*	201936_s_at			64	2.3
0.0035	0.5	235616_at	*235616_at*	235616_at			65	2.6
0.0036	1.9	Metallothionein 1X	*MT1X*	204326_x_at		PCR	66	2.6
0.0036	2.7	Peroxiredoxin 5	*PRDX5*	1560587_s_at			67	2.7
0.0037	0.3	Core-binding factor, runt domain, α subunit 2; translocated to, 2	*CBFA2T2*	207625_s_at			68	2.7
0.0037	0.4	Transcribed locus, moderately similar to XP_531878.2		230168_at			69	2.7
0.0038	0.3	Zinc finger protein 346	*ZNF346*	236267_at			70	2.8
0.0038	2.0	Metallothionein 1H-like protein /// hypothetical protein LOC650610	*LOC645745 /// LOC650610*	211456_x_at			71	2.9
0.0039	0.2	Hypothetical protein DKFZp586I1420	*DKFZp586I1420*	213546_at			72	3.4
0.0039	2.0	Adrenergic, β-2-, receptor, surface	*ADRB2*	206170_at			73	3.5
0.0039	0.3	CTD-binding SR-like protein rA9	*KIAA1542*	234952_s_at			74	3.5
0.0039	2.6	Peroxiredoxin 5	*PRDX5*	222994_at			75	3.6
0.004	0.2	ATPase, H^+ transporting, lysosomal 42kDa, V1 subunit C1	*ATP6V1C1*	226463_at			76	3.8
0.004	8.0	XK, Kell blood group complex subunit-related family, member 8	*XKR8*	218753_at			77	3.8
0.004	0.3	Caspase 6, apoptosis-related cystein peptidase	*CASP6*	242323_at			78	4.0
0.0041	0.4	Coagulation factor XII (Hageman factor)	*F12*	205774_at			79	4.0
0.0041	0.3	Centaurin, γ 2	*CENTG2*	240758_at			80	4.2
0.0042	0.6	LR8 protein	*LR8*	220532_s_at			81	4.2
0.0042	0.2	WD repeat domain 42A	*WDR42A*	243318_at			82	4.5
0.0042	2.6	Potassium channel tetramerisation domain containing 14	*KCTD14*	219545_at			83	4.7
0.0043	2.8	6-Phosphogluconolactonase	*PGLS*	218388_at			84	4.9
0.0044	3.8	Bruno-like 6, RNA binding protein (*Drosophila*)	*BRUNOL6*	227775_at			85	4.9
0.0044	2.3	Zinc finger protein 415	*ZNF415*	205514_at			86	5.0
0.0045	0.5	HIR histone cell cycle regulation defective homolog A (*S. cerevisiae*)	*HIRA*	240451_at			87	5.1
0.0046	0.5	Cardiolipin synthase 1	*CRLS1*	241741_at			88	5.9
0.0046	0.3	c-mer proto-oncogene tyrosine kinase	*MERTK*	233079_at			89	6.1
0.0047	0.2	Additional sex combs like 2 (*Drosophila*)	*ASXL2*	218659_at			90	6.5
0.0047	3.6	Platelet endothelial aggregation receptor 1	*PEAR1*	228618_at			91	6.9
0.0047	0.3	Core-binding factor, runt domain, α subunit 2; translocated to, 2	*CBFA2T2*	238549_at			92	7.4
0.005	0.6	Lysosomal associated protein transmembrane 4 β	*LAPTM4B*	208029_s_at			93	8.0

Pass, number of overlapped probes; PCR, the genes that were subsequently examined using real-time RT-PCR.

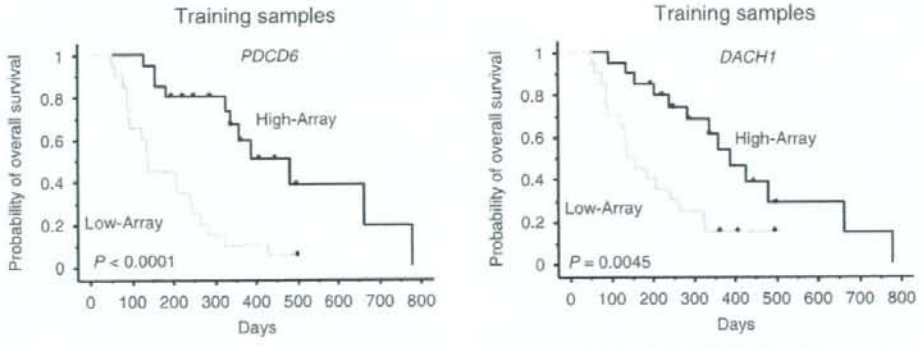

Fig. 2. Results of microarray data and patient survival in the training set of 40 patients. The Kaplan–Meier method was used for *DACH1* and *PDCD6*. The patients were divided into high and low expression groups by median values. The low *PDCD6* and *DACH1* expression groups had significantly poorer outcomes ($P < 0.0001$ and $P = 0.0045$). High-Array, group with high expression levels as determined by signal intensity of microarray data. Low-Array, group with low expression levels as determined by signal intensity of microarray data.

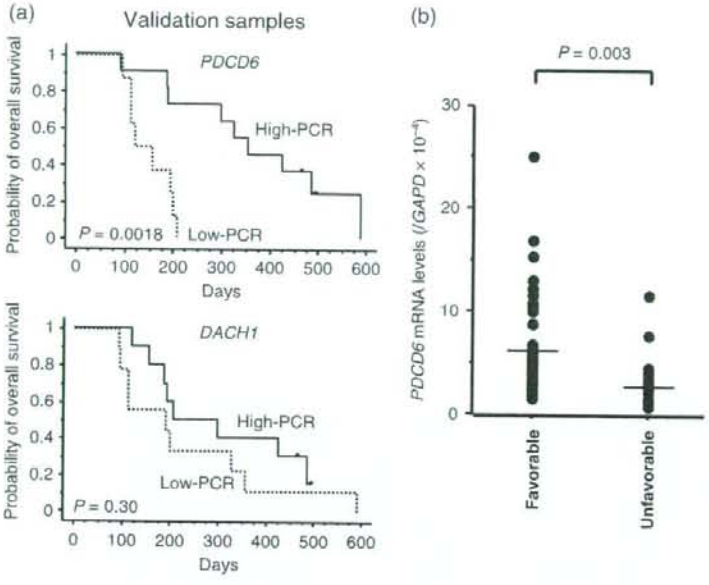

Fig. 3. Results of real-time reverse transcription polymerase chain reaction (RT-PCR) analysis and patient survival in the independent validation set of 19 samples. (a) The Kaplan–Meier method was used to estimate the overall survival. The low *PDCD6* expression groups had significantly poorer outcomes ($P = 0.0018$). High-PCR, group with high expression levels as determined by PCR. Low-PCR, group with low expression levels as determined by PCR. (b) All quantified expression levels of real time RT-PCR data are shown. The mRNA expressions of *PDCD6* were significantly lower in unfavorable group ($P = 0.003$) and varied ~25 fold (range, 0.98–25.1). Favorable, the patients with survival time over 180 days. Unfavorable, the patients with a survival time less than 180 days.

Table 3. Multivariate analysis of prognosis-related genes

Variable	Hazard ratio	95% confidence interval	*P*-value
Age (≥65)	1.78	0.570–5.559	0.3212
Sex (male)	3.26	0.732–14.489	0.1210
Performance status (≥1)	2.36	0.687–8.078	0.1728
Metastasis (≥3)	1.58	0.450–5.561	0.4739
Chemotherapy (5-FU)	1.48	0.402–5.475	0.5541
DACH1	0.38	0.175–0.817	0.0134
EGFR	1.41	0.992–2.001	0.0553
MT1X	0.71	0.317–1.600	0.4111
YWHAE	1.91	0.401–9.061	0.4169
GPX3	1.62	0.869–3.007	0.1293
PDCD6	0.06	0.010–0.334	0.0015
WDR33	1.38	0.268–7.067	0.7017
C14orf43	0.64	0.122–3.407	0.6045
MYLIP	0.67	0.221–2.042	0.4826
GKAP1	2.31	0.751–7.106	0.1440

Cox regression model was performed for multivariate analysis against each of the variables.

Table 4. Results of real-time *RT-PCR* for *PDCD6* and *DACH1* in an independent valiation set

Genes	Hazard ratio	95% confidence limits		*P*-value
		Upper	Lower	
*PDCD6**	0.29	0.12	0.71	0.007
DACH1	0.79	0.56	1.13	0.199

*, $P < 0.05$.

the uncontrollable factors, we aimed to avoid controllable factors with our best efforts. In this sense, we believe that the present study has succeeded in stratifying potential controllable variables.

Based on the results of the series of analyses conducted in the current study, we validated *PDCD6* as a molecular biomarker of the prognosis in gastric cancer.

PDCD6, also known as ALG-2 (apoptosis-linked gene-2), was first identified in a study on T-cell apoptosis conducted by Vito *et al.*[29] *PDCD6* encodes a calcium-binding protein that belongs to the penta-EF-hand protein family. The gene product participates in T-cell receptor-, Fas- and glucocorticoid-induced programmed cell death and cell proliferation. The stimulation of cells to enter the cell cycle is thought to drive the cellular apoptotic program, and the presence of additional survival or pro-apototic signals determines whether a cell proliferates or commits suicide. Krebs *et al.* indicated that the deregulation of such an obviously delicate balance could lead to pathological developments, such as cancer.[30] Detailed biological function of *PDCD6* genes in gastric cancer is still unclear. The speculated function may lead us to hypothesize that the expression is generally downregulated in cancer.

Our ultimate goal is to use real-time RT-PCR or immunohistochemical examination to identify patients with a poor prognosis prior to undertaking chemotherapy. We are now planning a large-scale prospective study based on the evidence obtained in the current study.

In conclusion, we identified prognostic biomarkers in patients with unresected gastric cancer, and our PCR-based single gene prediction strategy successfully predicted the overall survival of patients with gastric cancer. Our findings may provide a novel insight into the treatment of gastric cancer and may lead to a better understanding of this disease subgroup.

Acknowledgments

This work was supported by funds for the Third Term Comprehensive 10-Year Strategy for Cancer Control, a Grant-in-Aid for Scientific Research and the program for promotion of Fundamental Studies in Health Sciences of the National Institute of Biomedical Innovation (NiBio). The following people have played very important roles in the conduct of this project: Hiromi Orita, Hisanao Hamanaka, Ayumu Goto, Hisateru Yasui, Junichi Matsubara, Natsuko Okita, Takako Nakajima,

doi: 10.1111/j.1349-7006.2008.00935.x

Atsuo Takashima, Kei Muro, Takashi Ura, Hideko Morita, Mari Araake, Hisao Fukumoto, Tatsu Shimoyama, Naoki Hayama, Masayuki Takeda, Hideharu Kimura, Kazuko Sakai, Terufumi Kato and Jun-ya Fukai. We also thank Dr Richard Simon and Dr Amy Peng for providing us with the BRB ArrayTools software. This free software was very useful and has been developed for user-friendly applications.

References

1 Sastre J, Garcia-Saenz JA, Diaz-Rubio E. Chemotherapy for gastric cancer. *World J Gastroenterol* 2006; **12**: 204–13.
2 Vanhoefer U, Rougier P, Wilke H *et al.* Final results of a randomized phase III trial of sequential high-dose methotrexate, fluorouracil, and doxorubicin versus etoposide, leucovorin, and fluorouracil versus infusional fluorouracil and cisplatin in advanced gastric cancer: a trial of the European Organization for Research and Treatment of Cancer Gastrointestinal Tract Cancer Cooperative Group. *J Clin Oncol* 2000; **18**: 2648–57.
3 Ohtsu A, Shimada Y, Shirao K *et al.* Randomized phase III trial of fluorouracil alone versus fluorouracil plus cisplatin versus uracil and tegafur plus mitomycin in patients with unresectable, advanced gastric cancer: The Japan Clinical Oncology Group Study (JCOG9205). *J Clin Oncol* 2003; **21**: 54–9.
4 Sakata Y, Ohtsu A, Horikoshi N, Sugimachi K, Mitachi Y, Taguchi T. Late phase II study of novel oral fluoropyrimidine anticancer drug S-1 (1M tegafur-0.4M gimestat-1M otastat potassium) in advanced gastric cancer patients. *Eur J Cancer* 1998; **34**: 1775–20.
5 Koizumi W, Kurihara M, Nakano S, Hasegawa K. Phase II study of S-1, a novel derivative of 5-fluorouracil, in advanced gastric cancer. *Oncology* 2000; **58**: 191–7.
6 Shirao K, Shimada Y, Kondo H *et al.* Phase I–II study of irinotecan hydrochloride combined with cisplatin in patients with advanced gastric cancer. *J Clin Oncol* 1997; **15**: 921–7.
7 Boku N, Ohtsu A, Shimada Y *et al.* Phase II study of combination of irinotecan and cisplatin against metastatic gastric cancer. *J Clin Oncol* 1999; **17**: 319–23.
8 Boku N, Yamamoto S, Shirao K *et al.* Gastrointestinal Oncology Study Group/Japan Clinical Oncology Group. Randomized phase III study of 5-fluorouracil (5-FU) alone versus combination of irinotecan and cisplatin (CP) versus S-1 alone in advanced gastric cancer (JCOG9912) (Abstract). *Proc Am Soc Clin Oncol* 2007; **25**: 18S.
9 Chau I, Norman AR, Cunningham D, Waters JS, Oates J, Ross PJ. Multivariate prognostic factor analysis in locally advanced and metastatic esophago-gastric cancer – pooled analysis from three multicenter, randomized, controlled trials using individual patient data. *J Clin Oncol* 2004; **22**: 2395–403.
10 Metzger R, Leichman CG, Danenberg KD *et al.* ERCC1 mRNA levels complement thymidylate synthase mRNA levels in predicting response and survival for gastric cancer patients receiving combination cisplatin and 5-fluorouracil chemotherapy. *J Clin Oncol* 1998; **16**: 309–16.
11 Boku N, Chin K, Hosokawa K *et al.* Biological makers as a predictor for response and prognosis of unresectable gastric cancer patients treated with 5-fluorouracil and cis-platinum. *Clin Cancer Res* 1998; **4**: 1469–74.
12 Yonemura Y, Ninomiya I, Yamaguchi A *et al.* Evaluation of immunoreactivity for erbB-2 protein as a marker of poor short term prognosis in gastric cancer. *Cancer Res* 1991; **51**: 1034–8.
13 Sanz-Ortega J, Steinberg SM, Moro E *et al.* Comparative study of tumor angiogenesis and immunohistochemistry for p53, c-ErbB2, c-myc and EGFr as prognostic factors in gastric cancer. *Histol Histopathol* 2000; **15**: 455–62.
14 Shibata A, Parsonnet J, Longacre TA *et al.* CagA status of *Helicobacter pylori* infection and p53 gene mutations in gastric adenocarcinoma. *Carcinogenesis* 2002; **23**: 419–24.
15 Okusa Y, Ichikura T, Mochizuki H. Prognostic impact of stromal cell-derived urokinase-type plasminogen activator in gastric carcinoma. *Cancer* 1999; **85**: 1033–8.
16 Linder N, Haglund C, Lundin M *et al.* Decreased xanthine oxidoreductase is a predictor of poor prognosis in early-stage gastric cancer. *J Clin Pathol* 2006; **59**: 965–71.
17 Resnick MB, Gavilanez M, Newton E *et al.* Claudin expression in gastric adenocarcinomas: a tissue microarray study with prognostic correlation. *Hum Pathol* 2005; **36**: 886–92.
18 Kido S, Kitadai Y, Hattori N *et al.* Interleukin 8 and vascular endothelial growth factor – prognostic factors in human gastric carcinomas? *Eur J Cancer* 2001; **37**: 1482–7.
19 Xiangming C, Natsugoe S, Takao S *et al.* The cooperative role of p27 with cyclin E in the prognosis of advanced gastric carcinoma. *Cancer* 2000; **89**: 1214–9.
20 Yasui W, Oue N, Ono S, Mitani Y, Ito R, Nakayama H. Histone acetylation and gastrointestinal carcinogenesis. *Ann NY Acad Sci* 2003; **983**: 220–31.
21 Oue N, Motoshita J, Yokozaki H *et al.* Distinct promoter hypermethylation of p16INK4a, CDH1, and RAR-beta in intestinal, diffuse-adherent, and diffuse-scattered type gastric carcinomas. *J Pathol* 2002; **198**: 55–9.
22 Yamanaka R, Arao T, Yajima N *et al.* Identification of expressed genes characterizing long-term survival in malignant glioma patients. *Oncogene* 2006; **25**: 5994–6002.
23 Hasegawa S, Furukawa Y, Li M *et al.* Genome-wide analysis of gene expression in intestinal-type gastric cancers using a complementary DNA microarray representing 23 040 genes. *Cancer Res* 2002; **62**: 7012–17.
24 Hippo Y, Taniguchi H, Tsutsumi S *et al.* Global gene expression analysis of gastric cancer by oligonucleotide microarrays. *Cancer Res* 2002; **62**: 233–40.
25 Inoue H, Matsuyama A, Mimori K, Ueo H, Mori M. Prognostic score of gastric cancer determined by cDNA microarray. *Clin Cancer Res* 2002; **8**: 3475–9.
26 Leung SY, Yuen ST, Chu KM *et al.* Expression profiling identifies chemokine (C-C motif) ligand 18 as an independent prognostic indicator in gastric cancer. *Gastroenterology* 2004; **127**: 457–69.
27 Leung SY, Chen X, Chu KM *et al.* Phospholipase A2 group IIA expression in gastric adenocarcinoma is associated with prolonged survival and less frequent metastasis. *Proc Natl Acad Sci USA* 2002; **99**: 16203–8.
28 Chen CN, Lin JJ, Chen JJ *et al.* Gene expression profile predicts patient survival of gastric cancer after surgical resection. *J Clin Oncol* 2005; **23**: 7286–95.
29 Vito P, Lacana E, D'Adamio L. Interfering with apoptosis: $Ca^{(2+)}$-binding protein ALG-2 and Alzheimer's disease gene ALG-3. *Science* 1996; **271**: 521–5.
30 Krebs J, Saremaslani P, Caduff R. ALG-2: a Ca^{2+}-binding modulator protein involved in cell proliferation and in cell death. *Biochim Biophys Acta* 2002; **1600**: 68–73.

Novel SN-38–Incorporated Polymeric Micelle, NK012, Strongly Suppresses Renal Cancer Progression

Makoto Sumitomo,[1] Fumiaki Koizumi,[2] Takako Asano,[1] Akio Horiguchi,[1] Keiichi Ito,[1] Tomohiko Asano,[1] Tadao Kakizoe,[3] Masamichi Hayakawa,[1] and Yasuhiro Matsumura[4]

[1]Department of Urology, National Defense Medical College, Tokorozawa, Saitama, Japan; [2]Shien-Lab, Medical Oncology, National Cancer Center Hospital; [3]National Cancer Center, Tokyo, Japan; and [4]Investigative Treatment Division, Research Center for Innovative Oncology, National Cancer Center Hospital East, Chiba, Japan

Abstract

It has been recently reported that NK012, a 7-ethyl-10-hydroxy-camptothecin (SN-38)–releasing nanodevice, markedly enhances the antitumor activity of SN-38, especially in hypervascular tumors through the enhanced permeability and retention effect. Renal cell carcinoma (RCC) is a typical hypervascular tumor with an irregular vascular architecture. We therefore investigated the antitumor activity of NK012 in a hypervascular tumor model from RCC. Immunohistochemical examination revealed that Renca tumors contained much more CD34-positive neovessels than SKRC-49 tumors. Compared with CPT-11, NK012 had significant antitumor activity against both bulky Renca and SKRC-49 tumors. Notably, NK012 eradicated rapid-growing Renca tumors in 6 of 10 mice, whereas it failed to eradicate SKRC-49 tumors. In the pulmonary metastasis treatment model, an enhanced and prolonged distribution of free SN-38 was observed in metastatic lung tissues but not in nonmetastatic lung tissues after NK012 administration. NK012 treatment resulted in a significant decrease in metastatic nodule number and was of benefit to survival. Our study shows the outstanding advantage of polymeric micelle-based drug carriers and suggests that NK012 would be effective in treating disseminated RCCs with irregular vascular architectures. [Cancer Res 2008;68(6):1631–5]

Introduction

Passive targeting of the drug delivery system is suited to combating the pathophysiologic characteristics present in many solid tumors: hypervascularity, irregular vascular architecture, potential for secretion of vascular permeability factors, and the absence of effective lymphatic drainage that prevents efficient clearance of macromolecules. These characteristics, unique to solid tumors, are believed to be the basis of the enhanced permeability and retention (EPR) effect (1). Polymeric micelle-based anticancer drugs have recently been developed (2, 3), and some were put under evaluation for clinical trials (4, 5).

7-Ethyl-10-hydroxy-camptothecin (SN-38), a biological active metabolite of irinotecan hydrochloride (CPT-11), has potent antitumor activity, but has not been used clinically because it is a water-insoluble drug. It has been recently shown that novel SN38-incorporated polymeric micelles, NK012, have the potential to allow effective sustained release of SN-38 inside a tumor and possess potent antitumor activities especially in a vascular endothelial growth factor (VEGF)–secreting hypervascular tumor (6), because the supramolecular structures of NK012 which enable SN-38 to accumulate in the target tissue are based on the EPR effect (1).

Renal cell carcinoma (RCC) is a typical hypervascular tumor with an irregular vascular architecture. We therefore conducted an investigation to determine whether NK012 would be effective in treating RCC by using established RCC tumor models with pulmonary metastasis.

Materials and Methods

Drugs and cells. CPT-11 was purchased from Yakult Honsha Co., Ltd. SN-38 and NK012 was prepared and supplied by Nippon Kayaku Co., Ltd. (6). Five human RCC lines (SKRC-49, Caki-1, 769P, 786O, and KU19-20) and murine Renca cells were maintained in DMEM or MEM supplemented with 2 mmol/L glutamine, 1% nonessential amino acids, 100 units/mL streptomycin and penicillin, and 10% FCS.

***In vitro* growth inhibition assay.** The growth inhibitory effects of NK012, SN-38, and CPT-11 were examined with a 3-(4, 5-dimethylthiazol-2-yl)-2, 5-diphenyltetrazolium bromide (MTT) assay, as described previously (6).

***In vivo* growth inhibition assay.** The animal experimental protocols were approved by the Committee for Ethics of Animal Experimentation, and the experiments were conducted in accordance with the Guidelines for Animal Experiments in the National Cancer Center. Athymic nude mice (3–4 wk old) were maintained in a laminar air flow cabinet under aseptic conditions. 10^7 RCC cells were s.c. injected into the backs of the mice. NK012 at doses of 10 mg/kg/d or 20 mg/kg/d and CPT-11 at doses of 15 mg/kg/d or 30 mg/kg/d were given i.v. on days 0 (when tumors were allowed to grow until they became massive in size, around 1.5 cm), 4, and 8. Tumor volume was determined by direct measurement with calipers and calculated as $\pi/6 \times (\text{large diameter}) \times (\text{small diameter})^2$.

Assessment of treatment effects of NK012 on murine pulmonary metastasis model. A total of 1×10^5 Renca cells were inoculated into male BALB/c mice via the tail vein. The mice were randomly divided into three groups of 10. NK012 at dose of 20 mg/kg/d and CPT-11 at dose of 30 mg/kg/d were given i.v. on days 0 (7 d after inoculation), 4, and 8. After that, the mice were sacrificed, their lungs were stained intratracheally with 15% India black ink solution, and the number of metastatic nodules in each mouse was counted. To determine the effect of NK012 on survival, an identical experiment to the one described above was done. After treatment, mice were maintained until each animal showed signs of morbidity (i.e., over 10% weight loss compared with untreated controls), at which point they were sacrificed. Kaplan-Meier analysis was done to determine the effect on time to morbidity, and statistical differences were ranked according to a Mantel-Cox log-rank test using the StatView 5.0 software package.

Histologic and immunohistochemical analysis. Histologic sections were taken from Renca tumor tissues. After extirpation, tissues were fixed with 3.9% formalin in PBS (pH 7.4), and the subsequent preparations and H&E staining were performed by Tokyo Histopathological Laboratory Co.,

Requests for reprints: Yasuhiro Matsumura, Investigative Treatment Division, Research Center for Innovative Oncology, National Cancer Center Hospital East, 6-5-1 Kashiwanoha, Kashiwa City, Chiba 277-8577, Japan. Phone: 81-4-7134-6857; Fax: 81-4-7134-6857; E-mail: yhmatsum@east.ncc.go.jp.

doi:10.1158/0008-5472.CAN-07-6532

Table 1. *In vitro* growth inhibitory activity of SN-38, NK012, and CPT-11 in RCC lines (MTT assay)

Cell line	IC_{50} (μmol/L)		
	SN-38	NK012*	CPT-11
SKRC-49	0.0064 ± 0.005	0.011 ± 0.008	4.14 ± 0.45
Caki-1	0.0062 ± 0.009	0.032 ± 0.006	8.45 ± 0.85
769P	0.015 ± 0.007	0.085 ± 0.014	34.54 ± 3.76
786O	0.031 ± 0.007	0.12 ± 0.012	28.14 ± 1.21
KU19-20	0.10 ± 0.006	0.34 ± 0.014	32.65 ± 1.25
Renca	0045 ± 0.005	0.0096 ± 0.008	2.26 ± 0.05

*The dose of NK012 is expressed as a dose equivalent to SN-38.

Ltd. Monoclonal anti-CD34 antibody (HyCult Biotechnology) was used to detect the tumor blood vessels. CD34-positive neovessels were counted in 10 high-power fields (×400) by two independent investigators who operated in a blinded fashion.

Assay for free (polymer-unbound) SN-38 in lung tissues. The Renca pulmonary metastasis model described above was used for the analysis of the biodistribution of NK012 and CPT-11. Ten days after Renca inoculation, NK012 (20 mg/kg) or CPT-11 (30 mg/kg) was given i.v. to the mice. The mice were sacrificed at 0, 24, 48, and 72 h after administration, and lung samples were taken and stored at −80°C until analysis. We prepared control mice without Renca inoculation as the nonmetastatic model; NK012 was administrated as well, and lung samples were stored. Samples were then homogenized on ice using a Digital homogenizer (Iuchi) and suspended in the mixture of 100 mmol/L glycine-HCl buffer (pH 3)/methanol (1:1, v/v) at a concentration of 5% w/w. Proteins were precipitated with an ice-cold mixture of 1 mmol/L H_3PO_4/MeOH/H_2O (1:1:4, v/v/v) containing camptothecin as an I.S. The sample was vortexed for 10 s and filtered through a MultiScreen Solvinert (Millipore Corporation), and the concentration of free SN-38 in the aliquots of the homogenates (100 μL) was determined using the high-performance liquid chromatography method (6).

Statistical analysis. Data were expressed as mean ± SD. Significance of differences was calculated using the unpaired *t* test with repeated measures of StatView 5.0. $P < 0.05$ was regarded as statistically significant.

Results and Discussion

We first evaluated *in vitro* cellular sensitivity of RCC lines to SN-38, NK012, and CPT-11. The IC_{50} values of each agent for RCC lines are shown in Table 1. NK012 exhibited higher cytotoxic effect against each cell line compared with CPT-11 (96-fold to 406-fold sensitive).

It is essential to elucidate the correlation between the effectiveness of micellar drugs and tumor hypervascularity and hyperpermeability. Gross evaluation of those RCC tumors s.c. injected into the backs of mice revealed that Renca tumors were more reddish and grew faster than SKRC-49 tumors, and immunohistochemical examination showed that Renca tumors contained much more CD34-positive neovessels than SKRC-49 tumors (Fig. 1).

We allowed the tumors to grow until they became massive, around 1.5 cm, and then initiated treatment. A striking decrease in Renca tumor volume was observed on day 15 in mice treated with NK012 at 20 mg/kg/d compared with the untreated control (Fig. 2*A*). Renca bulky masses completely disappeared on day 21 in 6 of 10 mice treated with NK012 at 20 mg/kg/d. On the other hand, Renca tumors in mice treated with CPT-11 at 30 mg/kg/d were not eradicated and rapidly regrew after a partial response at day 15. An approximate 10% body weight loss occurred in mice treated with NK012 20 mg/kg, compared with the untreated controls, but there was no significant difference in comparison with tumor-free mice treated with NK012, suggesting that the decrease in body weight was likely to be due to tumor shrinkage rather than toxic effects. We next compared the antitumor activities of the NK012 and CPT-11 treatment in SKRC-49 and Renca tumors. The SKRC-49 tumor volume in mice treated with NK012 at 20 mg/kg/d on day 21 was over 70% smaller than in the untreated controls on day 21 and ~50% smaller than in mice on day 0 (Fig. 2*B*). However, the SKRC-49 tumors were not eradicated in mice treated with NK012. Considering that equivalent *in vitro* growth inhibitory effects by NK012 were observed for SKRC-49 and Renca cells (Table 1), our results suggest that the antitumor activity of NK012 *in vivo* might be affected by tumor environment factors, such as tumor vascularity.

We next examined the distribution of free SN-38 in the metastatic or nonmetastatic (no inoculation of Renca cells) lung tissues after administration of NK012 or CPT-11. In the case of NK012 administration in mice with lung metastasis, free SN-38 was detectable at the concentration of >100 ng/g in metastatic lung tissues with a typical microvascular architecture (Fig. 3*A*) even at 72 hours after administration, whereas the concentrations of free SN-38 in nonmetastatic lung tissues after NK012 administration were much lower than those in metastatic lung tissues after treatment with NK012 (significant at 24, 48, and 72 hours; $P < 0.05$;

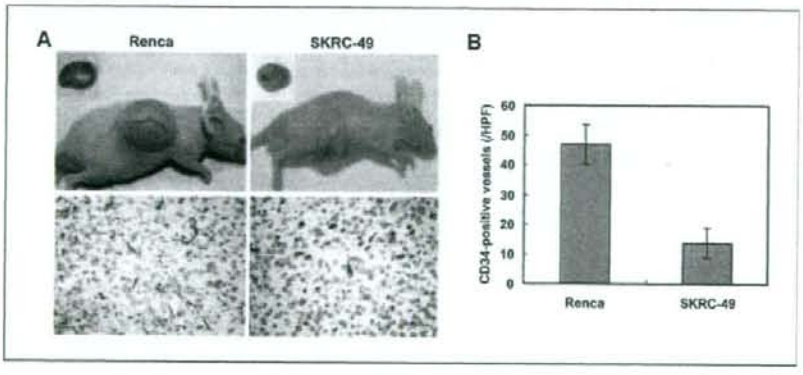

Figure 1. Comparison of tumor angiogeneses of Renca and SKRC-49 in athymic nude mice. *A*, representative photographs of massive tumors developed from Renca and SKRC-49 at 28 d after s.c. injection (inoculation). Immunohistochemical (CD34, ×400) examinations for each tumor are shown. *B*, tumor neovascularization in each tumor was quantified by counting CD34-positive neovessels. *Bars*, SD. Experiments were repeated twice with similar results.